Universita Karlova

Faculty of Science
Department of Inorganic Chemistry

Polycyclic tetraazamacrocycles

Ph.D. Thesis

Jan Plutnar

Kladno/Prague 2007

Table of contents

Chapter One

Introduction

1.1 General Introduction

The largest group of compounds used as ligands for radio-copper complexation is built on tetraazamacrocycles, containing from 12 to 14 atoms in a single ring. The synthesis of these compounds is relatively facile and thermodynamic and kinetic properties of the obtained copper complexes are often suitable for use in radiodiagnostic or radiotherapeutic methods. In recent years, an intensive research on a field of polycyclicpolyazamacrocycles have been undertaken in sense of ligand synthesis and coordination chemistry investigation. The results have shown up e.g. much improved kinetic stability of transition metal complexes in comparison with the complexes of monocyclic ligands.

1.2. Topologically constrained azamacrocycles

Bridging superstructures added to small azamacrocycles* enhance the characteristic that makes azamacrocycles indispensable ligands for transition metal coordination chemistry – high complex stability. Addition of a few-atom-bridge connecting at least two nitrogen atoms of the macrocycle changes the shape of the molecule making it more rigid in space and possibly increases the stability of a complex with metal ion.

1.2.1 Chelate effect -> Macrocyclic effect -> Cryptate effect

The characteristics present in macrocycles leading to their uncommonly stable metal complexes are now fairly well understood, and can be grouped together under the term 'molecular organization'.[1] The two major areas of molecular organization, as related to coordination chemistry, are complementarity and constraint factors. Complementarity, the sum of size, geometry, and electronics matching between the metal ion and the ligand is conceptually the simplest of these two to understand and manipulate (since there are a finite number of metal ions, donor types, geometries, and useful ligand sizes, it is apparent, that for a given metal ion, the complementarity of a ligand can be maximized). The metal-ligand binding can be further increased only through the exploitation of the second area – the constraint factors. Constraint is concerned with the number and flexibility of the connections between the donor atoms of the ligand. The ligand rigidity and complexity can be manipulated to produce jumps in complex stability (compared with the ligand systems that lack them).

The linking of two donor atoms together results in a chelate. Such a linkage causes a large increase in the binding constants with the metal ions (compared with the separate donor groups). There are various explanations of this phenomenon.[2],[3],[4] The common thermodynamic rationalization for the chelate

*for the purpose of this text small azamacrocycles are tetraazacycles

effect points out the increase in entropy associated with chelate binding (compared with the binding of separate monodentate donors). This arises because the total number of particles in the system increases during the complexation reaction. An additional effect is the increased effective concentration of the next donor, because the distance from the metal ion is fixed by the link to the bound preceding donor.[2] This distance is short compared with an unlinked second donor, whose average distance from the metal ion depends primarily on its concentration. A reasonable support for this effect is that the formation of the second metal-donor atom bond is abnormally fast (compared with an unlinked second donor). On the other hand, the dissociation of the individual donors (in a flexible chelate) is as fast as that for a corresponding monodentate ligand.[5]

Tying successive donor atoms together produces tri- or tetradentate chelates and further increases the metal complex stability as a function of the number of chelate rings (Fig.1.1).[1] But another jump in stabilization appears when the terminal donor atoms of a linear polydentate ligand are linked to form a ring. This phenomenon was termed macrocyclic effect.[6]

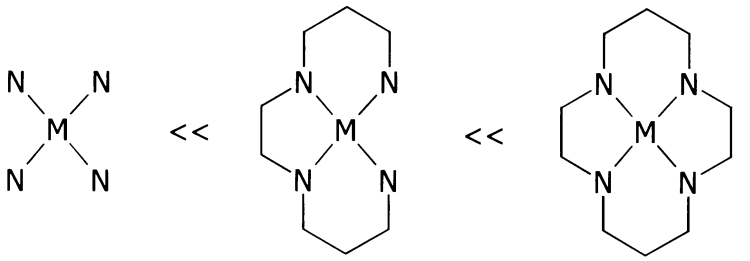

Fig.1.1 – Relative stability of complexes with equal number of donor atoms of the same type

An accepted explanation of the macrocyclic effect lies in a difficult dissociation of the first donor atom from the metal ion in a stepwise dissociation of the polydentate ligand. A polydentate linear chelating ligand can dissociate from a metal ion through successive S_N1 replacement steps, the cascade starting on a terminal donor atom. On the contrary, the macrocyclic chelating ligand cannot dissociate through a similarly simple mechanism because there is no terminal donor atom. At first, some kind of ligand rearrangement must occur to weaken one metal-donor atom bond prior to its dissociation (this costs some energy making the dissociation slow). This primarily dissociative effect is a supplement to the highly associative chelate effect, which is still in effect for macrocycles. Combinations of these effects results in the large increase in stabilization for macrocyclic complexes.

A further extension of topological constraint is the cryptate effect, in which the addition of the second ring to a macrocycle (leading to the bicyclic ligand)

further increases the stability of its metal complexes.[7] Similarly to the chelate -> macrocyclic effect transition, the cryptate effect is often higher than would be expected for a simple addition of the second fused macrocycle. The exact origin of this effect is not yet agreed upon, but there is an obvious connection between the increasing topological constraint and the binding affinity. The bicyclic (or, more generally, polycyclic) ligand has much more rigid structure than the similar monocyclic one thus making stepwise donor atom dissociation even much slower than in case of the latter one.[8] An additional concept called preorganization[9] was developed to describe the observation that ligands preformed in a size and geometry complementary to the metal ion, had higher stabilities with this ion than other ligands and this concept fits well the behaviour of macrobicyclic ligands.

1.2.2 Synthesis of polycyclic azamacrocycles

Nitrogen-containing polycyclic macrocycles are well known and have been synthesised and investigated for many years and many purposes.[1],[10] Probably the most famous are the cryptands (e.g. **1**, Fig.1.2), which were synthesised[11] by a high-dilution bridging reaction to improve the binding ability of crown ether ligands for alkali and alkaline earth metal ions. Yet other examples are the clathrochelates[12] and sepulchrates[13], that may be viewed as tetraaza-macrocycles spanned by a bis-donor bridge connected to carbon bridgehead atoms of the ring (e.g. **2**, Fig.1.2). These ligands provide a unprecedented stability for some metal ions of good secondary amine complementarity by filling all coordination sites and having the topology necessary for the cryptate effect.[14]

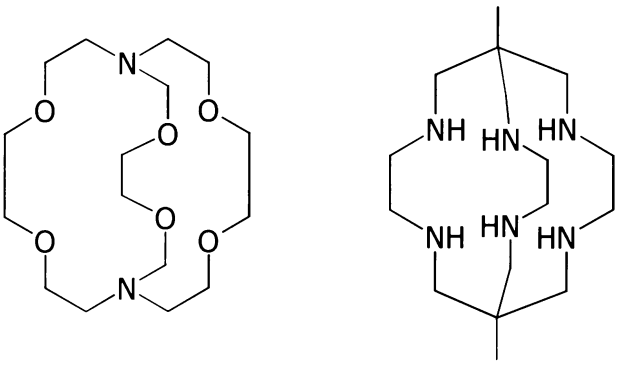

1 **2**

Fig.1.2 – Example of cryptand (**1**) and sepulchrate (**2**)

There could be many other examples of macro-polycyclic ligands found in the literature but the following text is focused on the ligands containing four nitrogen atoms and where the bridging part of the molecule connects these heteroatoms.

1.2.2.1 Direct organic synthesis

One of the simplest methods how to introduce two-carbon bridges between nitrogen atoms of cyclam (or cyclen)* is reaction of the macrocycle with dibromomethane, leading to both mono- and di-bridged macrocycles (Scheme 1.1).[15] This method has also been adapted for the production of larger, 'side-bridged' tetraazamacrocycles (**3** and **4** Fig.1.3).[16]

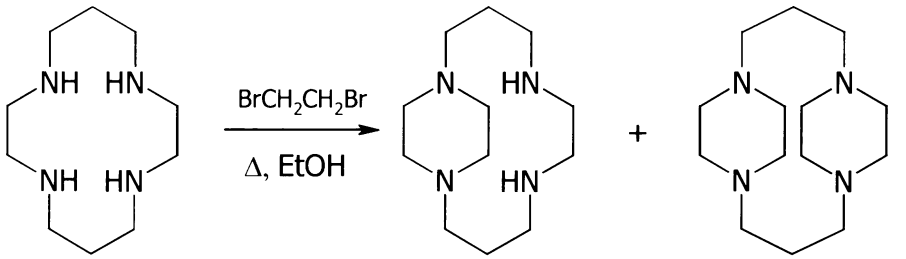

Scheme 1.1 – Bridging alkylation of cyclam

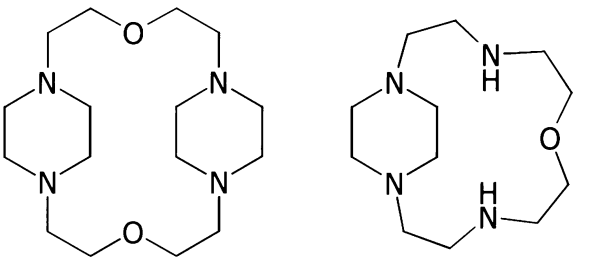

3 **4**

Fig.1.3 – Large structurally reinforced macrocycles

Use of another bridging agent, diethyl oxalate, produces a bis-amide side-bridged macrocycle that can be reduced to give products similar to the ligands described in Scheme 1.1 (Scheme 1.2).[17] These ligands can be further modified by substitution of the remaining secondary amino nitrogen atoms to alter their complexation properties.[18],[19]

1.2.2.2 Template-directed synthesis

Template-directed synthesis is the organization of an assembly of atoms with respect to one or more geometric points to achieve a particular linking of atoms.[20] For the synthesis of macrocyclic ligands, metal ions are utilized as the 'anchors' of the template complexes. The template-directed synthesis of the simple monocyclic ligand was well developed[21] and further extended to produce e.g. ethylene 'side-bridged' 15-membered macrobicyclic ligand (Scheme 1.3).[22]

* cyclam = 1,4,8,11-tetraazacyclotetradecane, cyclen = 1,4,7,10-tetraazacyclododecane

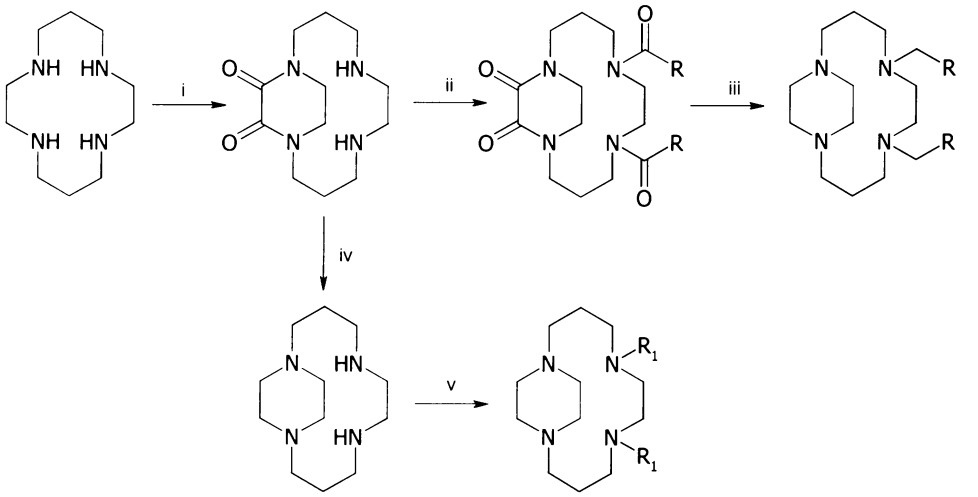

i) EtOC(=O)C(=O)OEt; ii) RC(=O)Cl; iii, iv) $BH_3 \cdot SMe_2$, THF; v) R^1Br, base, MeCN

Scheme 1.2 – Synthesis and modification of mono 'side-bridged' cyclam

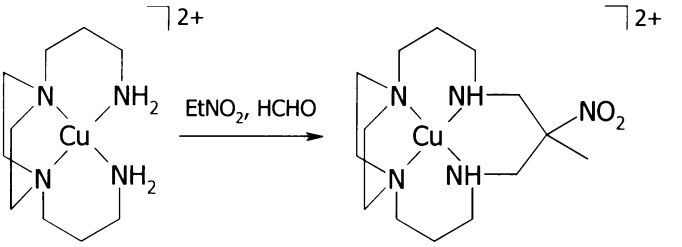

Scheme 1.3 – Template closure of a 'side-bridged' macrocycle

The main advantages of this approach are the ease and high yield of the reactions. Additionally, a pendant donor (through further reduction of the NO_2 group) is added to the macrocycle, forming a potentially pentadentate ligand coming across e.g. in the Co^{3+} complex.[22] Ligands similar to that in Scheme 1.3 were produced by template reactions involving *N,N'*-bis(aminoalkyl)-1,4-diazacycloheptanes as the starting materials in place of the piperazine starting materials. The nickel(II)-templated reactions of these tetraamines produced several 'side-bridged' ligands which can be described as ethylene bridged across propylene-separated adjacent nitrogens of various macrocycles (Fig.1.4).[23]

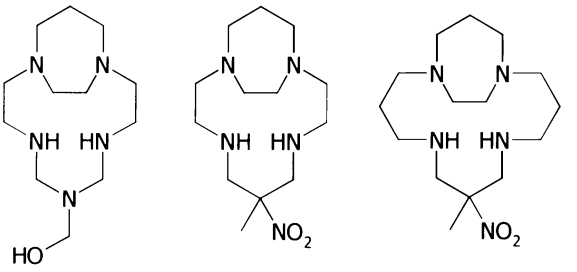

5 **6** **7**

Fig.1.4 – 1,4-Diazacycloheptane-containing bicyclic ligands

In summary, it is apparent that direct and template syntheses work best for bridging adjacent nitrogen atoms in azamacrocycles, producing 'side-bridged' polycyclic compounds. However, only few cross-bridged ligands have been obtained by these methods. These piperazine- or 1,4-diazacycloheptane based macrocycles are, in terms of rigidity, less effective ligands than the 'cross-bridged' tetraazamacrocycles. Although the adjacent nitrogens atoms are very rigidly separated, the rest of the macrocycle, a quite lengthy unbridged portion, is little affected. The major part of the ligand is still relatively flexible, and the full advantages of rigidification through bridging are not realized.

1.2.2.3 Synthesis using selective substitution and protective groups

In case where the direct syntheses or template-directed methods fail to produce the desired compound, selective substitution and protection/ deprotection of functional groups has been applied. Such an example is the series of ligands based on 1,7-Me_2cyclen, which are prepared by classical macrocyclization method[24] from the disodium salt of *N'*-methyl-*N,N''*-bis (toluene-*p*-sulphonyl)diethylenetriamine and bis(2-chloro-ethyl)methylamine (Scheme 1.4).[25]

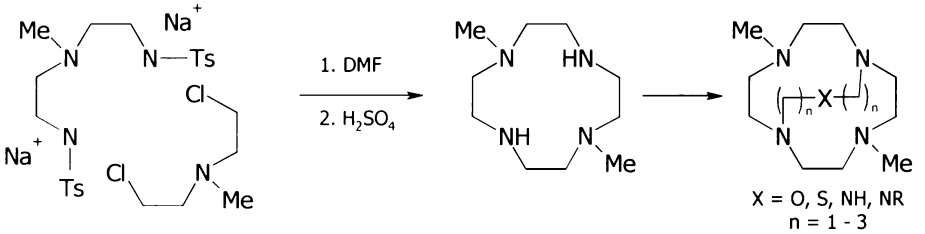

Scheme 1.4 – Synthesis of cyclen-based macrobicycles

Another protection/deprotection bridging synthesis uses amides as protecting groups to set a cross-bridge cyclam.[26] The *trans* dioxocyclam starting material (1,4,8,11-tetraazacyclotetradecane-5,12-dione),[27] is a product of Michael addition involving ethylenediamine and methyl acrylate. Two aromatic groups,

1,3-bis(bromomethyl)benzene or 2,6-bis(bromomethyl)pyridine, have been used to cross-bridge the *trans* protected macrocycle under high-dilution conditions. Borane reduction in tetrahydrofuran resulted in 'deprotection' by conversion of the two amides to amines (Scheme 1.5).

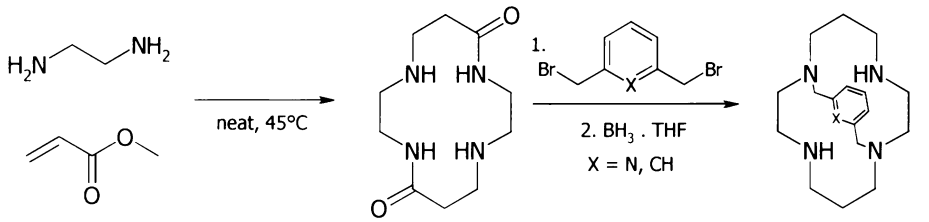

Scheme 1.5 – Synthesis of 'cross-bridged' cyclam via *trans*-dioxocyclam

Regioselective, stoichiometric, *trans* bis-tosylation of cyclen allows substitution of the two remaining nitrogen atoms by bis-*O*-tosylated 1,3-propanediol. Deprotection, followed by a repeated bridging step, results in the spherical doubly-bridged compound (Scheme 1.6).[28],[29] A similar procedure, starting with mono-*N*-tosylated 1,4,7-triazacyclononane, yields an analogous compound containing two ethylene bridges ('hexaethylenetetraamine', **8**, Fig.1.5).[30] A direct reaction between a triazamacrocycle and a trifunctional bridging group produces another similarly symmetric tricyclic compound containing only propylene (trimethylene) bridges ('hexapropylenetetraamine', **9**, Fig.1.5).[31] Due to the rigid arrangement of nitrogen atoms lone pairs directed into the cavity, all these ligands behave as proton sponges.

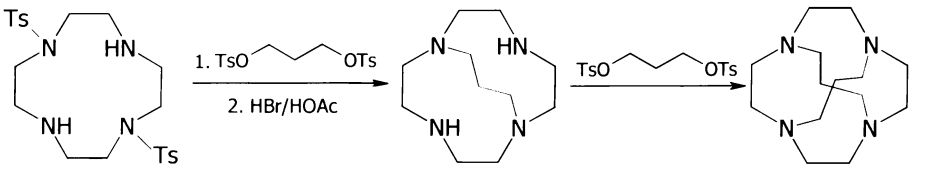

Scheme 1.6 – Synthesis of propylene bis-cross-bridged cyclen

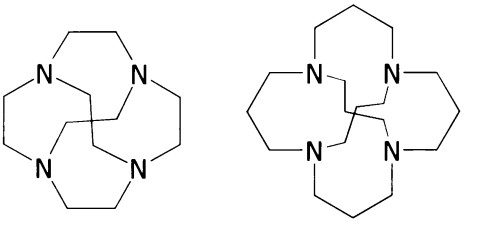

8 **9**

Fig.1.5 – Highly symmetric proton sponges

Many other nitrogen-bridged bicyclic ligands have been prepared, mostly containing bipyridine or phenanthroline bridges. They are often larger and contain more nitrogen donor atoms than four that the text is focused to. Their syntheses are generally similar to the syntheses of cryptands where the

polyether chains are replaced by bipy or phen groups. The produced large ligands have mostly been used for alkali and alkaline earth metal ions complexation or, in some cases, for lanthanide(III) ions complexation.[32]

1.2.2.4 Condensation synthesis

Synthesis of bridged azamacrocycles via condensation of monocyclic compound with an aldehyde is one of the most used and the easiest (in terms of number of steps) methods for syntheses of these compounds.

Condensation of an aldehyde with two amines to form aminal functional groups is well known; one of the oldest examples is the condensation of formaldehyde with ammonia to form hexamethylenetetraamine (urotropine).[33] Similar reactions of formaldehyde with tetraazamacrocycles yield compounds with single carbon atom bridges between adjacent nitrogen atoms.[34] Although these compounds have not been exploited for transition metal coordination, some of them can be used as starting materials for preparation of selectively nitrogen-substituted monocyclic azamacrocycles (Scheme 1.7).[35]

Similarly, the condensation of cyclam with dimethyl acetal of DMF (dmfdma) yields a *cis*-bridged (diprotected) cyclam that can be used for preparation of 1,11-disubstituted cyclam derivatives (Scheme 1.8).[36]

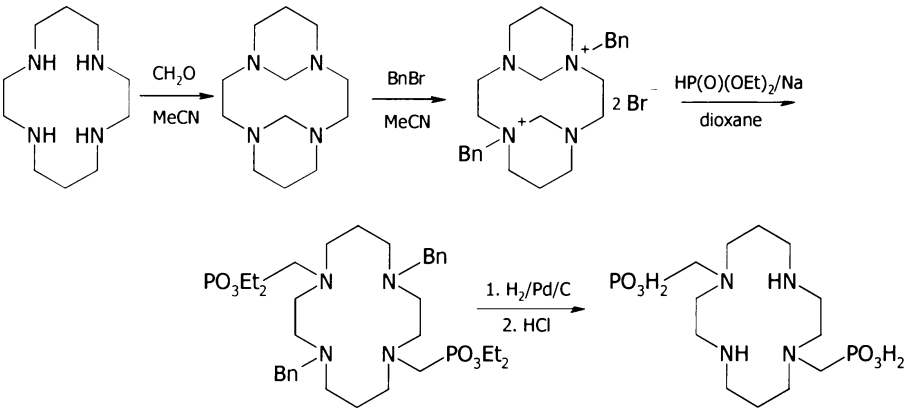

Scheme 1.7 – Synthesis of 1,8-disubstituted cyclam derivative via cyclam-formaldehyde aminal

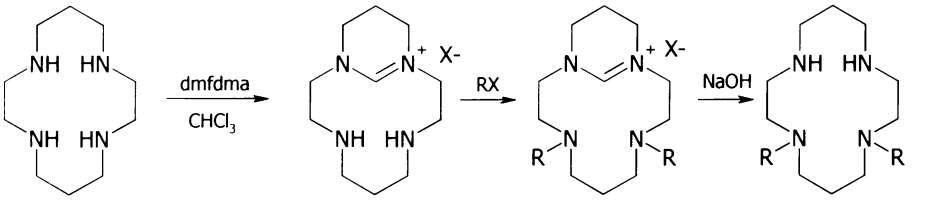

Scheme 1.8 – Synthesis of 1,11-disubstituted cyclam derivative

During condensation of tetraazamacrocycle with glyoxal each aldehyde functional group reacts with two secondary amines of the macrocycle, giving a tetracyclic molecule.[37] This tetracyclic compound has been used as precursors to either the side-bridged[38] or cross-bridged tetraazamacrocycles (Scheme 1.9).[39]

Condensation of glyoxal with two equivalents of diamine (1,3-diaminopropane), followed by further formaldehyde condensation, yields smaller tetracyclic macrocycle (**10**, Fig.1.6).[40]

Another interesting 'tetraaminal' is a [2+2] condensation product of glyoxal and diethylenetriamine (**11**, Fig.1.6).[41]

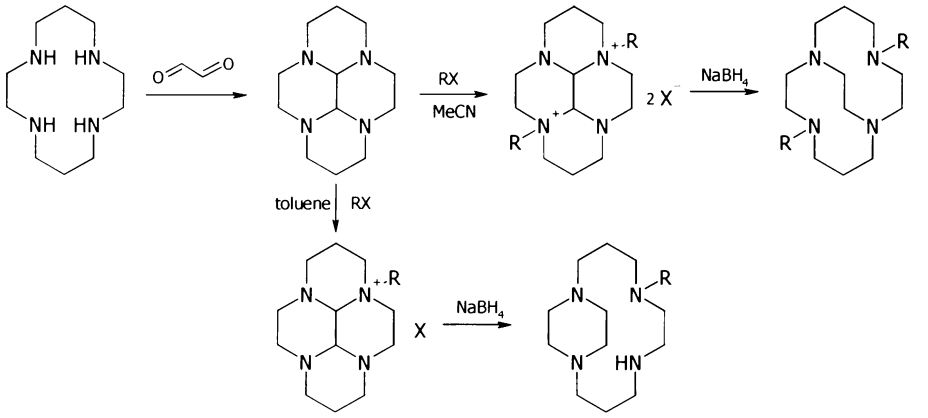

Scheme 1.9 – Cyclam-glyoxal bisaminal as a starting material for synthesis of bridged macrocycles

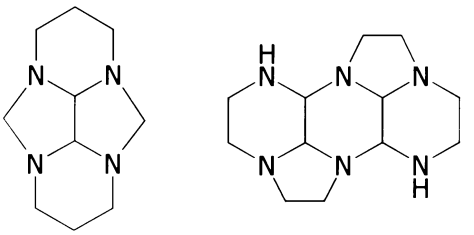

10 **11**

Fig.1.6 – Condensation product of glyoxal and formaldehyde with linear polyamines

As can be seen, there are many possible pathways to the polyaza-polymacrocycles which, as will be shown below, can have interesting coordination properties. As this work is primarily focused on tetraaza-macrocycles built on the cyclam skeleton, only metal ion complexes with this family of ligands will be further reviewed.

1.2.3 Structures and properties of polycyclic tetraazamacrocycles

The polycyclic tetraazamacrocycles may be divided into two subgroups according to the number of rings in the molecule – tricyclic tetraamines containing two nitrogen-nitrogen bridges and bicyclic tetraamines with one bridging chain. These groups may be further divided into another subgroups with side-bridged or cross-bridged macrocycles.

1.2.3.1 Side-bridged macrocycles

The side-bridged macrocycles are products of a simple reaction between an unsubstituted monocyclic azamacrocycle and either formaldehyde (introducing the methylene bridge, cf. Ch. *1.2.2.4*) or a difunctional alkylating agent (e.g. 1,2-dibromoethane introducing the ethylene bridge, cf. Ch. *1.2.2.1*).
The methylene bridged polycycles have not been exploited for the transition metal ion coordination, since it is believed that the one-carbon bridges would prevent the coordination of both connected nitrogen atom from binding the same central atom.[42] The solid-state structure of the bis-methylene-bridged cyclam have been determined,[43] showing the *trans* orientation of the CH_2 bridges and confirming the unsuitability of the compound for a single metal ion coordination (Fig.1.7).

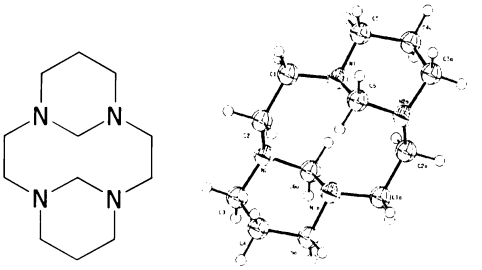

Fig.1.7 – Schematic diagram and the ORTEP view of bis-methylene-bridged cyclam (50% probability thermal ellipsoids)

While the solid-state structure of the bis-ethylene-bridged macrocycle (Scheme 1) is not known and no transition metal coordination chemistry of this compound have been reported, the structure of the mono-ethylene-bridged derivative have been determined[44],[58] and its coordination chemistry comprising several metals ions (Cr^{III}, Ni^{II}, $Cu^{I,II}$) has been explored.[44],[45],[46] The solid-state structure of the free ligand possesses a chair conformation of the piperazine ring[58] and an unusual twisted-boat (twist) conformation of the piperazine ring in the triprotonated form of the amine,[44] which changes to the more common boat-like ring in its metal complexes (Fig.1.8, 1.9).

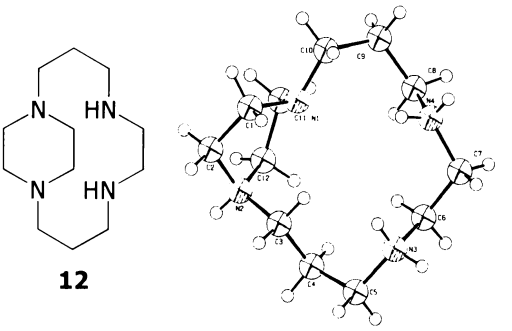

12

Fig.1.8 – Schematic diagram of the ethylene-side-bridged cyclam and the molecular structure of its triprotonated form (50% probability thermal ellipsoids)

The demetallation kinetics of the copper(II) complex of **12** in acidic solution have been investigated,[44] showing kinetic inertness of the complex being similar to that of the cyclam-copper complex ($t_{½}$ ~ 22 days for the cyclam complex vs. $t_{½}$~23.5 days for the side-bridged complex, in 1M $HClO_4$ at 60 °C). Although the detailed mechanism for the demetallation process have not been proposed, it is supposed that the reason for this unexpected behaviour lies in the structural change between the coordinated and 'free' ligand. The results of semiempirical calculations (PM3) of various piperazine conformers show that the twist form has lower total energy than the boat conformer and that the conformational change is not affected by any energy barrier (the process is spontaneous). Since under the conditions of the decomplexation experiment the uncoordinated macrocycle is present in the triprotonated form, the conformational change from the boat conformer in the coordinated form to the twist form in the free ligand makes the decomposition of the complex easier.

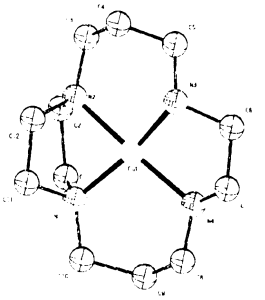

Fig.1.9 – ORTEP view of Cu^{II}-complex of **12**
(50% probability thermal ellipsoids, hydrogen atoms and anions are omitted for clarity)

1.2.3.2 Cross-bridged macrocycles

Introduction of ethylene or propylene (trimethylene) bridge(s) to the non-adjacent nitrogen atoms of a tetraaza macrocyclic ligand generates so called

cross-bridged macrocycle. The bicyclic (or tricyclic) macrocycles are sometimes named bowl-adamanzanes (or cage-adamanzanes),[47] referring to the overall shape of the molecules.

1.2.3.2.1 Cages

The oldest example of cage-like tricyclic tetraamine is hexamethylene-tetraamine whose crystal structure was the first structure of an organic compound obtained by X-ray diffraction.[48] In this compound the nitrogen atoms lone pairs are directed outwards the cavity. In larger macrocycles, starting with hexaethylenetetraamine (**8**, Fig.1.5) through ligands with varying numbers of ethylene/propylene bridges to the hexapropylenetetraamine (**9**, Fig.1.5), these lone pairs are directed towards the inside of the cavity, giving the compounds some interesting acid/base properties. The cages are obtained in inside- monoprotonated forms and it seems very likely that the proton is encapsulated during the synthesis of the ligand.[30] In fact, there are some observations showing that the syntheses of the cage-like ligands are template-assisted with a coordinated proton being the template or serving as the protecting group.[47]

The presence of the proton inside the cavity have been proven by several experiments, using independent methods comprising ^{1}H NMR and IR spectroscopy. E.g. the highly symmetric macrocycle **8** (Fig.1.5) shows two signals in proton NMR spectra assigned to the encapsulated hydrogen atom and the ethylene -CH_2- groups with H-H splitting 1.0 Hz caused by coupling with the encapsulated proton, reflecting the T_d symmetry of the molecule in solution.[30] However, in the solid state, the proton seems to be located on one of the four identical nitrogen atoms (although the proton have not been located on the difference Fourier map, the results of the N···N distances comparison point out to the protonated nitrogen atom).[30] Generally, the chemical shift of the encapsulated proton varies from 9.8 to 15.2 ppm for different cage-like tetraaza-macrotricycles. The DFT calculations gave chemical shift values for the proton which are in excellent agreement with the observed ones.[49]

The encapsulation of the inside proton by the organic framework of the tricyclic compounds may explain their extreme robustness. The half-life for the H/D exchange reaction in 1M NaOH is reported to be longer than 1 year ($k_{ex} < 10^{-8}$ s^{-1}). Many experiments have shown that even the treatment with strong base such as butyllithium or reducing agent such as $NaBH_4$ in aprotic, organic solvents did not deprotonate the compound.[47] In addition, the reaction of sodium metal with glycolate of cage-like macrocycle **9** (Fig.1.5) in liquid ammonia leads to production of an 'inverse sodium hydride' in form of golden crystals, stable in the solid state up to –25 °C.[50]

From the statements given above it is obvious that the usability of this kind of cross-bridged azamacrocycles in transition metal coordination chemistry is negligeable or even zero.

1.2.3.2.2 Bowls

The overall shape of the bowl-like tetraazamacrocycles is well suitable for coordination of proton or a transition metal ion. In aqueous media, the pK_a values of many mono-protonated amines are greater than 13, in case of propylene bridged cyclen **13** (Fig.1.10) greater than 15;[51] for the monoprotonated ethylene-bridged cyclam derivative **14** (Fig.1.10) the pK_a value in non-aqueous media (acetonitrile) is equal to 24.9.[39] Another common feature is the extreme acidity of the tetraprotonated species with pK_{a1} values commonly below 2 (in case of **13** below –1).[47]

The metal coordination chemistry of the bowl-like ligands is interestingly rich and a large number of coordination compounds have been reported, including metal ions $Cu^{I,II}$, Ni^{II}, $Co^{II,III}$, $Fe^{II,III}$, $Mn^{II,III}$, Ga^{III}, In^{III}, Pd^{II} and Zn^{II}. The coordination geometries vary from tetrahedral through square pyramidal and trigonal bipyramidal to octahedral environments. In all structures the ligands coordinate through at least the four nitrogen atoms, even in the structure of Pd^{II} complex of **14**, where the palladium(II) ion adopts an unusual five-coordinated square-pyramidal geometry.[52]

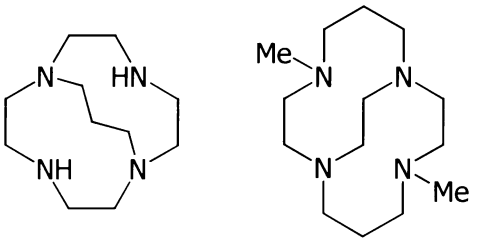

13 **14**

Fig.1.10 – Examples of cross-bridged tetraazamacrocycles with extreme acid/base properties

For copper(II), the complexes with octahedral, trigonal bipyramidal, square pyramidal and many intermediate arrangements between the latter two geometries have been described. The copper(II) complex of bis(*N*-benzylated) ethylene-cross-bridged cyclam is an example of complex with distorted trigonal-bipyramidal environment (derived from an octahedron by removal of one equatorial ligand) characteristic for many five-coordinated complexes of bowl-like azamacrocycles (Fig.1.11).[53] The Cu^{II} complex with bis(*N*-carbamoylmethyl) derivative of the same macrocycle possesses an octahedral coordination sphere (Fig.1.12).[54]

One of the most important features of the cross-bridged tetraazamacrocycles is their extraordinary inertness with respect to cleavage of the metal ion from the macrobicycle. In aqueous hydrochloric acid the complexes slowly decompose to form hexaaqua ions (or the tetrachlorometallate anions) and the corresponding protonated amine.[47]

An example of such reaction in 5 M HCl is given below (Eq.1):[47]

$$[Cu(\mathbf{13})Cl]^{+} + 3H^{+} + n Cl^{-} \rightarrow [CuCl_{(n+1)}]^{(n-1)-} + H_3(\mathbf{13})^{3+} \qquad \text{Eq.1}$$

The reaction follows first-order kinetics with $k_{cleavage}$ = 1.48 x 10^{-6} s^{-1}. The corresponding reaction of $[Cu(cyclen)^{2+}]$ in 5 M HCl is much faster, $k_{cleavage}$ = 0.72 s^{-1}.[47] The kinetic data of several copper(II) complexes are given in Table 1. Unfortunately, no kinetic study upon cyclam-based cross-bridged azamacrocycles are available except a partial study on Cu^{II} complex of **14**,[55] showing extreme kinetic stability in acidic media ($k_{cleavage}$ = 3.5 x 10^{-9} s^{-1} at 40 °C in 1 M $HClO_4$).

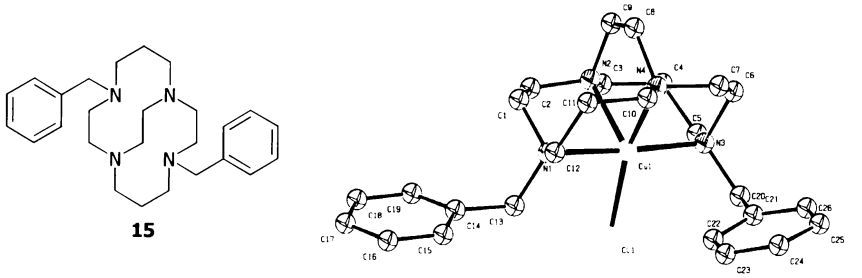

15

Fig.1.11 – Ligand **15** and the molecular structure of its complex $[Cu(\mathbf{15})Cl]Cl \cdot H_2O$ (30% probability thermal ellipsoids, anion, solvate molecule and hydrogen atoms are omitted for simplicity)

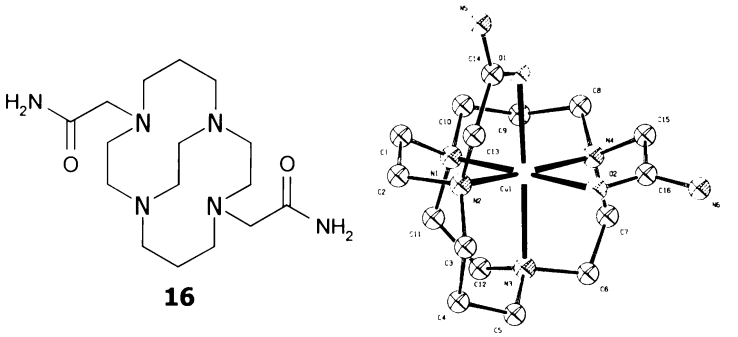

16

Fig.1.12 – Ligand **16** and the molecular structure of its complex in $[Cu(\mathbf{16})](NO_3)_2 \cdot MeOH \cdot H_2O$ (30% probability thermal ellipsoids, anions, solvate molecules and hydrogen atoms are omitted for simplicity)

Table 1.1 – Kinetic parameters for the metal extrusion in 5 M HCl at 25 °C[56]

	$k_{cleavage}$ [s^{-1}]	$\Delta H^{\neq}$ [kJ/mol]	$\Delta S^{\neq}$ [J/mol·K]
[Cu(**13**)Cl]$^+$	1.48(2) x 10^{-6}	89(6)	–60(14)
[Cu(**17**)Cl]$^+$	1.79(5) x 10^{-6}	93(4)	–42(9)
[Cu(**18**)Cl]$^+$	2.28(6) x 10^{-7}	121(4)	32(14)

For structures of **17** and **18** see Fig.13 below

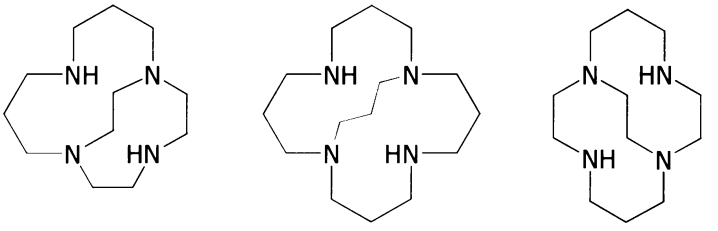

17 **18** **19**

Fig.1.13 – Ligands referred to in Table 1 and 2

1.2.4 Radiocopper-labelled bicyclic macrocycles

The Cu^{II} complexes of cyclam-based bicyclic tetraaza-macrocyclic ligands show thermodynamic stability parameters similar to the Cu-cyclam complex (cf. Table 1.2). Unfortunately, in addition to the lack of kinetic data for the complexes of the cyclam-derived compounds no further thermodynamic data (except those in Table 1.2) could be found in the literature. Especially, the absence of any data for the di-N-substituted derivatives is elusive.

Table 1.2 – Thermodynamic stability constants for Cu^{II} complexes

ligand	*log* K_{Cu-L}	*reference*
cyclam	28.09	[57]
12	26.1	[58]
19	27.1	[59]

Conditions: 25°C, μ=0.1 M KCl, for structure of ligand **19** see Fig.1.13

Despite the lack of either thermodynamic or kinetic data, several studies of *in vivo* behaviour of the copper(II) complexes have been carried out and the data compared with the analogous monocyclic complexes. While the unsubstituted cross-bridged bicyclic complexes show behaviour similar to the cyclam complex,[58],[59] the di-*N*-substituted derivatives (Fig.1.14) possess e.g. higher stability in rat serum (*in vitro*; no detectable decomposition up to 24 h).[59] The ^{64}Cu complex of **20** (Fig.1.14) was found to be more resistant to transchelation than ^{64}Cu-TETA in rat liver metabolism studies. In addition, this

complex demonstrated very rapid clearance through blood, liver and kidney (in normal rats), suggesting a significant potential of bifunctional ligands built on **20** for binding copper radionuclides to biological molecules for diagnostic imaging.[59] The copper(II) complexes of the other two ligands **21** and **22**, respectively, exhibit rapid uptake in the liver and kidneys with a slow clearance, probably due to their overall positive charge.

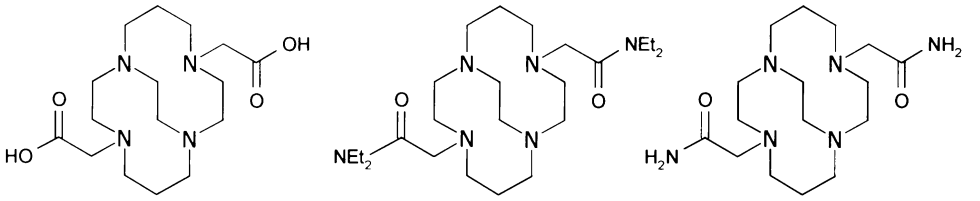

20 **21** **22**

Fig.1.14 – Bicyclic ligands used in *in vivo* radiolabelling experiments

1.2.5 Bifunctional bicyclic chelates

There are several possible chemical pathways for delivery of a radio-nuclide to the living organism. Related to polyazamacrocyclic ligands, the bifunctional chelator approach is the most frequently used one. Many mono-cyclic bifunctional chelators have been prepared and have been used in common radiopharmaceuticals (cf. Appendix I). Reports of bicyclic bifunctional chelators preparations are very scarce, in fact only the synthesis and properties of one bicyclic bifunctional ligand have been reported (Fig.1.15).[60]

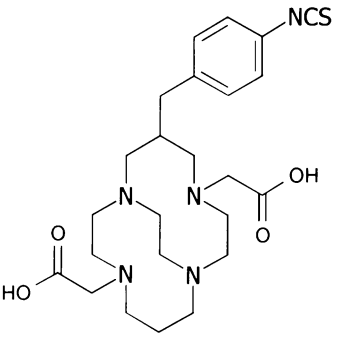

23

Fig.1.15 – The bifunctional bicyclic chelator

1.3. Conclusion

The aim of this work is to fill in the gap in bifunctional bicyclic chelators by preparation of non-symmetrically di-N-substituted tetraazabicycles, either side- or cross-bridged, and evaluation of their complexation properties considering their potential use as radiocopper chelators. In addition, a comparison of the

newly prepared ligands' metal complexes properties with the properties of complexes of the monocyclic, symmetrically substituted cyclam-based ligand 1,4,8,11-tetraazacyclotetradecane-1,8-bis(methylphosphinic acid) (1,8-H_4te2p), prepared and investigated independently, will be done.

References:

[1] D. H. Bush, *Chem. Rev.*, **1993**, *93*, 847
[2] G. Schwarzenbach, *Helv. Chim. Acta.*, **1952**, *35*, 2344
[3] E. L. Simmons, *J. Chem. Educ.*, **1979**, *56*, 578
[4] A. E. Martell, R. D. Hancock, R. J. Motekaitis, *Coord. Chem. Rev.*, **1994**, *133*, 39
[5] G. A. Melson, R. G. Wilkins, *J. Chem. Soc.*, **1963**, 2662
[6] D. K. Cabbiness, D. W. Margerum, *J. Am. Chem. Soc.*, **1969**, *91*, 6540
[7] J.-M. Lehn, J.-P. Sauvage, *J. Am. Chem. Soc.*, **1975**, *97*, 6700
[8] D. H. Busch, K. Farmery, V. Goedken, V. Katovic, A. C. Melnyk, C. R. Sperati, N. Tokel, *Adv. Chem. Ser.*, **1971**, *100*, 44
[9] D. J. Cram, M. P. de Grandpre, C. B. Knobler, K. N. Trueblood, *J. Am. Chem. Soc.*, **1984**, *106*, 3286
[10] W. P. Schammel, K. S. Bowman-Mertes, G. G. Christoph, D. H. Busch, *J. Am. Chem. Soc.*, **1979**, *101*, 1622
[11] B. Dietrich, J.-M. Lehn, J.-P. Sauvage, *Tetrahedron Lett.*, **1969**, 2885 and 2889
[12] D. R. Boston, N. J. Rose, *J. Am. Chem. Soc.*, **1968**, *90*, 6859
[13] I. I. Creaser, J. M. B. Harrowfield, A. J. Herlt, A. M. Sargeson, J. Springborg, *J. Am. Chem. Soc.*, **1977**, *99*, 3181
[14] A. M. Sargeson, *Pure Appl. Chem.*, **1986**, *58* , 1603
[15] K. P. Wainwright, *Inorg. Chem.*, **1980**, *19*, 1396
[16] M. Kodama, E. Kimura, S. Yamaguchi, *J. Chem. Soc. Dalton Trans.*, **1980**, 2536
[17] J. W. Krajewski, P. Gluzinski, R. A. Kolinski, A. Kemme, A. Mishnev., *Pol. J. Chem.*, **1994**, *68*, 703
[18] R. Kowallick, M. Neuburger, M. Zehnder, T. A. Kaden, *Helv. Chim. Acta*, **1997**, *80,* 948
[19] S. J. Archibald, E. A. Lewis, T. J. Hubin, *PCT WO 2005/121109 A2,* December 22nd, **2005**
[20] D. H. Busch, *J. Incl. Phenom.*, **1992**, *72*, 389
[21] P. Comba, N. F. Curtis, G. A. Lawrence, A. M. Sargeson, B. W. Skelton, A. H. White, *Inorg. Chem.*, **1986**, *25*, 4260
[22] L. M. Engelhardt, G. A. Lawrence, T. M. Manning, A. H. White, *Aust. J. Chem.*, **1989**, *42*, 1859
[23] R. D Hancock, M. P. Ngwenya, P. W. Wade, J. C. A. Boeyens, S. M. Dobson, *Inorg. Chim. Acta*, **1989**, *164*, 73
[24] J. E. Richman, T. J. Atkins, *J. Am. Chem. Soc.*, **1974**, *96*, 2268

[25] M. Ciampolini, M. Micheloni, N. Nardi, P. Paoletti, F. Zanobini, *J. Chem. Soc., Dalton Trans.*, **1984**, 1357
[26] F. Denat, S. Lacour, S. Brandes, R. Guilard, *Tetrahedron Lett.*, **1997**, *38*, 4417
[27] D. A. Tomalia, L. R. Wilson, *US Patent 4,517,122* , May 14th, 1985
[28] J. Springborg, P. Kofod, C. E. Olsen, H. Toflund, I. Søtofte, *Acta Chem. Scand.*, **1995**, *49*, 547
[29] J. Springborg, C. E. Olsen, I. Søtofte, *Acta Chem. Scand.*, **1995**, *49*, 555
[30] Y. Miyahara, Y. Tanaka, K. Amimoto, T. Akazawa, T. Sakuragi, H. Kobayashi, K. Kubota, M. Suenaga, H. Koyama, T. Inazu, *Angew. Chem. Int. Ed.*, **1999**, *38*, 956
[31] J. Springborg, U. Pretzmann, C. E. Olsen, *Acta Chem. Scand.*, **1996**, *50*, 294
[32] B. Alpha, E. Anklam, R. Deshenaux, J.-M. Lehn, M. Pietraskiewicz, *Helv. Chim. Acta*, **1988**, *71*, 1042
[33] A. T. Nielsen, D. W. Moore, M. D. Ogan, R. L. Atkins, *J. Org. Chem.*, **1979**, *44*, 1678
[34] R. W. Alder, E. Heilbronner, E. Honegger, A. B. McEwen, R. E. Moss, E. Olefirowicz, P. A. Petillo, R. B. Sessions, G. R. Weismann, J. M. White, Z.-Z. Yang, *J. Am. Chem. Soc.*, **1993**, *115*, 6580
[35] J. Kotek et al., unpublished results
[36] P. J. Davies, M. R. Taylor, K. P. Wainwright, *Chem. Commun.*, **1998**, 827
[37] P. W. R. Caulkett, D. Greatbanks, R. W. Turner, J. A. Jarvis, *J. Chem. Soc., Chem. Commun.*, **1977**, 1013
[38] R. Kolinski, *Pol. J. Chem.*, **1995**, *69*, 1039
[39] G. R. Weisman, M. E. Rogers, E. H. Wong, J. P. Jasinski, E. S. Paight, *J. Am. Chem. Soc.*, **1990**, *112*, 8604
[40] D. S. C. Black, D. C. Craig, O. Giitsidis, R. W. Read, A. Salek, M. A. Sefton, *J. Org. Chem.*, **1989**, *54*, 4771
[41] H. Strasdeit, W. Saak, S. Pohl, W. L. Driessen, J. Reedjik, *Inorg. Chem.*, **1988**, *27*, 1557
[42] N. W. Alcock, P. Moore, K. F. Mok, *J. Chem. Soc., Perkin Trans. II*, **1980**, 1186
[43] G. Royal, V. Dahaoui-Gindrey, S. Dahaoui, A. Tabard, R. Guilard, P. Pullumbi, C. Leconte, *Eur. J. Org. Chem.*, **1998**, 1971
[44] M. Doiocchi, M. Bonizzoni, L. Fabbrizzi, F. Foti, M. Licchelli, A. Poggi, A. Taglietti, M. Zema, *Chem. Eur. J.*, **2004**, *10*, 3209
[45] K. Wright-Garcia, J. Basinger, S. Williams, Ch. Hu, P. S. Wagenknecht, L. C. Nathan, *Inorg. Chem.*, **2003**, *42*, 4885
[46] R. Kowallick, M. Neuburger, M. Zehnder, T. A. Kaden, *Helv. Chim. Acta.*, **1997**, *80*, 948
[47] J. Springborg, *Dalton Trans.*, **2003**, 1653
[48] R. G. Dickinson, A. L. Raymond, *J. Am. Chem. Soc.*, **1923**, *45*, 22
[49] V. Galasso, *Chem. Phys.*, **2001**, *270*, 79

[50] M. Y. Redko, M. Vlassa, J. E. Jackson. A. W. Misiolek, R. H. Huang, J. L. Dye, *J. Am. Chem. Soc.*, **2002**, *124*, 5928
[51] S. Brandès, F. Denat, S. Lacour, F. Rabiet, F. Barbette, P. Pullumbi, R. Guilard, *Eur. J. Org. Chem.*, **1998**, 2349

[52] T. J. Hubin, N. W. Alcock, D. H. Busch, *Acta Crystallogr., Sect. C*, **1999**, *55*, 1404
[53] G. R. Weisman, E. H. Wong, D. C. Hill, M. E. Rogers, D. P. Reed, J. C. Calabrese, *J. Chem. Soc., Chem. Commun.*, **1996**, 947
[54] W. Niu, E. H. Wong, G. R. Weisman, L. N. Zakharov, C. D. Incarvito, A. L. Rheingold, *Polyhedron*, **2004**, *23*, 1019
[55] T. J. Hubin, N. W. Alcock, M. D. Morton, D. H. Busch, *Inorg. Chim. Acta*, **2003**, *348*, 33
[56] L. Broge, U. Pretzmann, N. Jensen, I. Søtofte, C. E. Olsen, J. Springborg, *Inorg. Chem.*, **2001**, *40*, 2323
[57] R. J. Motekaitis, B. E. Rogers, D. E. Reichert, A. E. Martell, M. J. Welch, *Inorg. Chem.*, **1996**, *35*, 3821
[58] T. M. Jones-Wilson, K. A. Deal, C. J. Anderson, D. W. McCarthy, Z. Kovacs, R. J. Motekaitis, A. D. Sherry, A. E. Martell, M. J. Welch, *Nucl. Med. Biol.*, **1998**, *25*, 523
[59] X. Sun, M. Wuest, G. R. Weisman, E. H. Wong, D. P. Reed, A. Boswell, R. Motekaitis, A. E. Martell, M. J. Welch, C. J. Anderson, *J. Med. Chem.*, **2002**, *45*, 469
[60] E. A. Lewis, R. W. Boyle, S. J. Archibald, *Chem. Commun.*, **2004**, 2212

>-----<

CHAPTER TWO

1,4-ethylene-bridged cyclam derivatives: Syntheses, crystal structures and solution studies

Abstract

A series of new compounds built up on the skeleton of 1,5,8,12-tetraazabicyclo-[10.2.2]hexadecane (1,4-ethylene-bridged cyclam, 1,4-en-cyclam) have been synthesised and characterised by means of NMR and MS spectroscopy and a single-crystal X-ray structure determination. The attempts to substitute the secondary amino group of the *p*-nitrobenzyl-1,4-en-cyclam **3**, using acetic acid derivatives as the alkylating agents, lead to unexpected substitution of one of the piperazine ring nitrogen atoms, yielding the monoquarternary derivatives **4** and **5**, respectively. In order to explain this reaction behaviour, the solution-structure of the starting compound **3** have been established using two-dimensional NMR techniques. Several copper(II) complexes of the ligands have also been prepared and characterised. The acid-base behaviour of the ligands, thermodynamic stability constants of their copper(II) complexes and the speciation in metal-ligand systems in water were determined using the potentiometric titrations.

2.1. Introduction

The synthesis of structurally constrained tetraazamacrocycles with two donor nitrogen atoms connected by an additional bridge is a constantly developing area of the chemistry of macrocycles. Although there are many papers concerning the synthesis and coordination properties of various kinds of the bridged azamacrocycles[1],[2] and the original synthetic pathway leading to 1,5,8,12-tetraazabicyclo[10.2.2]hexadecane (1,4-en-cyclam, **1**, Fig.2.1) is known for almost 30 years,[3] only a marginal attention has been given to its coordination properties[4] and to synthesis and coordination properties of its derivatives.[5],[6],*

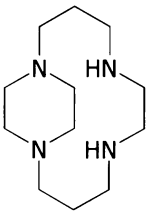

1

Fig.2.1 – Structure of 1,5,8,12-tetraazabicyclo[10.2.2]hexadecane (1,4-en-cyclam)

Substitution on the secondary amino nitrogen atoms of **1** by use of common alkylating or acylating agents in presence of a base leads to production of the symmetrically disubstituted derivatives. A different procedure starting with a monoquarternary salt of the cyclam-glyoxal condensation product results in production of unsymmetrical, monosubstituted macrocycle containing one secondary amino nitrogen available for further substitution.[5]

The aim of this work is the introduction of a functional group that may possibly improve some critical parameters of copper(II) complexes (i.e. the formation and decomplexation kinetics and the thermodynamic stability) and the study of properties of the newly prepared ligands and their Cu^{II} and Zn^{II} complexes.

2.2. Results and discussion

2.2.1 Synthesis

The general synthetic pathway leading to the monosubstituted 1,4-en-cyclam derivatives is shown in Scheme 2.1.[5],[7] The first synthetic step, the glyoxal-cyclam bisaminal preparation, consists in an addition of aqueous solution of glyoxal (1,2-ethanedione) to a cyclam suspension in acetonitrile. Although the reported bisaminal yields were reported to be good to excellent (> 80 %)[7] in the real experiment the yield does not exceed 50 %. One of the reasons of this result may be the composition of the commercially available 40 % w/w (6 M) aqueous glyoxal solution which is known to contain concentration- and

* recently two papers dealing with monosubstituted 1,4-en-cyclam derivatives have been published (ref.22)

temperature-dependent amounts of the reactive monomeric species, this amount being substantially lowered with the increasing total concentration (~11 % of the monomeric species in the 40 % aqueous solution) and the age of the material (oxidation on exposition to air).[8],[9]

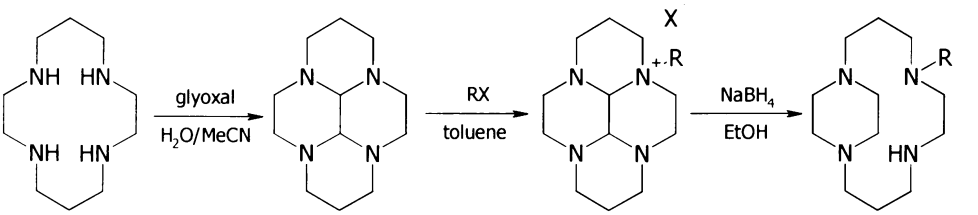

Scheme 2.1 – The reported synthesis of monosubstituted 1,4-en-cyclam derivatives

A suitable alternative source of glyoxal is its trimeric form. Dissolution of the trimer in hot distilled water (~70–80 °C) produces the solution, in which the hydrated glyoxal monomer (ethane-1,1,2,2-tetraol) predominates (see Ch. 2.2.2). This monomer reacts, after dilution by methanol, with cyclam to give the bisaminal in high and reproducible yields (~75–85 %).

Alkylation of the bisaminal intermediate in a suitable solvent produces the monoquarternary ammonium salt in form of a precipitate (toluene for R = benzyl, acetonitrile for R = *p*-nitrobenzyl). Reduction of a suspension of the ammonium salt in ethanol by a 20-fold excess of $NaBH_4$ in 5 days produces the desired 1,4-en-cyclam derivative.[5] It is possible to reduce the amount of the reducing agent used in the reaction either by conducting the reaction in methanol (10-fold excess of $NaBH_4$ is needed)[6] or in ethanol containing approx. 10 % of water (2-fold excess of the reductant). Use of the latter solvent also significantly reduces the time needed to complete the reaction (from 5 days to 8 hours).

Substitution of the secondary amino nitrogen of the monosubstituted 1,4-en-cyclam derivative has been attempted either by an alkylation reaction or by a Mannich-type reaction. Although the alkylation of similar derivatives in presence of an additional base has been reported,[6] alkylation of the *p*-nitrobenzyl-substituted compound by either ethyl bromoacetate or *tert*-butyl-bromoacetate in a polar solvent (e.g. acetonitrile) in presence of a base (K_2CO_3, Et_3N or $^iPr_2NEt$) leads to quantitative (based on amount of the alkylating agent) formation of the monoquarternised dialkylated compound **4** (Fig.2.2, Scheme 2.2).

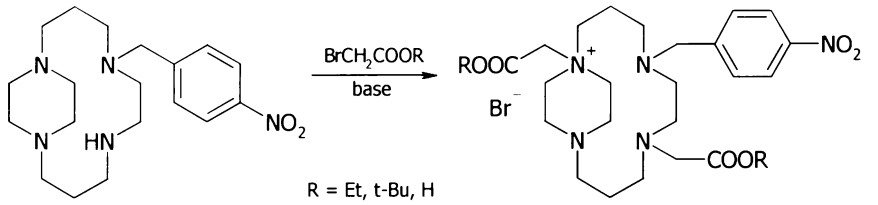

Scheme 2.2 – The undesirable overalkylation of the 1,4-en-cyclam derivative

All the alkylating agent is completely consumed during the reaction and the final mixture contains the dialkylated derivative **4**, the starting compound **3** and only a trace amount of the monoalkylated product, which was later identified as compound **5**. An attempt to substitute the secondary nitrogen atom of the macrocycle in a non-polar solvent, without presence of any additional base, unexpectedly yielded the monosubstituted quaternary compound **5** instead of the expected product **5a** (Scheme 2.3).

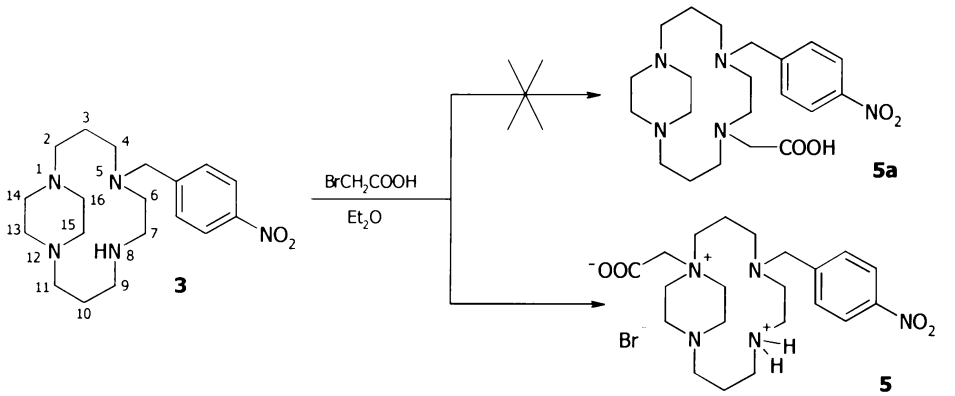

Scheme 2.3 – The unexpected quaternisation of the piperazine ring

The reasonable explanation of this behaviour could be found in the basicity of the secondary nitrogen atom of the starting compound **3**. This compound might have been isolated in its monoprotonated form as an ionic pair with hydroxide anion (see the experimental part). The relatively high basicity of the ligand **3** may facilitate existence of this ionic pair in benzene. According to the molecular mechanics (MM+) modelling results, the additional proton attached to the secondary nitrogen atom N8 would participate in the hydrogen bond system involving N12 and eventually N5 nitrogen atoms, thus deactivating these atoms for further electrophillic substitution. This hypothesis was confirmed by several homo- and heteronuclear 2D NMR measurements (see Ch. 2.2.2). The only nitrogen atom in such system available for further substitution is the N1 atom, which is too distant from the hydrogen bond system to participate in it. The alkylating agent attacks this nitrogen atom forming the 'tetraalkylammonium' quaternary centre. If the reaction proceeds in a non-polar solvent (e.g. diethyl ether) the product precipitates out of the reaction mixture in form of a yellow powder having the structure and composition shown in Scheme 2.3. In the reaction media with higher polarity (acetonitrile, water) and in presence of a base this molecule preferably reacts with further equivalent of the alkylating agent, forming the compound **4** (cf. Scheme 2.4). Reactivity of the secondary amine atom N8 of compound **5** must be significantly higher than the reactivity of the N1 nitrogen atom of the piperazine subunit in compound **3** as the final reaction mixture contains only a trace amount of the monoalkylated product **5** (detectable by the MS spectrometry) and a majority of the dialkylated compound **4**.

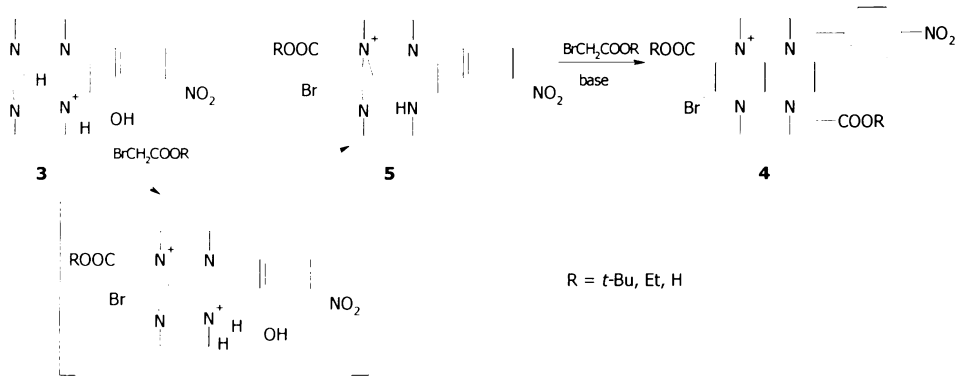

Scheme 2.4 – Proposed reaction pathway for stepwise alkylation of **3**

The methylphosphinate and methylphosphonate derivatives have been synthesised via Mannich-type reactions of the secondary amine, formaldehyde (in form of paraformaldehyde) and an appropriate acid (H_3PO_2) at ambient temperature (to produce a methylphosphinate) or an ester ($P(OEt)_3$) at elevated temperature (to produce a methylphosphonate) in low yields (~40 % of the estimated amount). Raising the temperature of the reaction mixture containing the phosphinic acid results in appearance of an inconsiderable amount of side-products, the most abundant among them being the hydroxymethylphosphinate ($HOCH_2(OH)(O)PCH_2N\sim$) derivative.

The products and intermediates prepared and characterised in this work are shown in Fig.2.2.

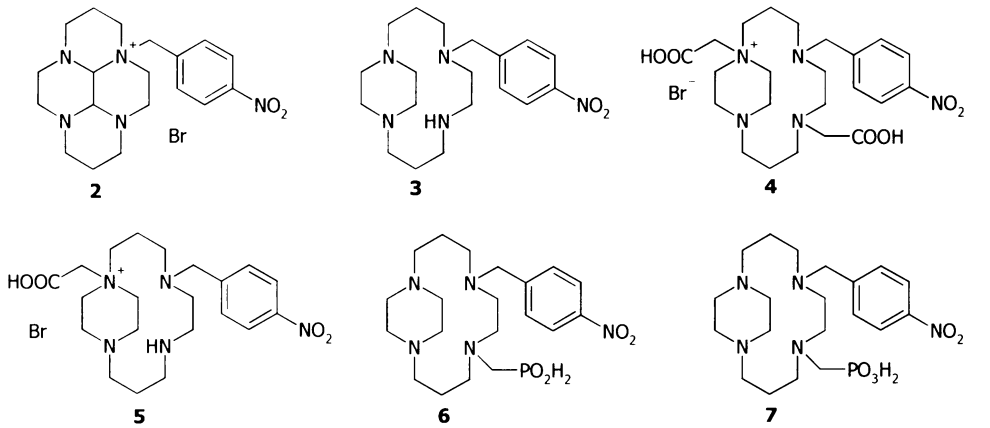

Fig.2.2 – Overview of compounds prepared in this work

2.2.2 NMR spectra

The ^{1}H NMR spectra of solutions prepared by dissolution of glyoxal hydrate trimer in water exhibit the line-structure similar to the spectra of commercially available glyoxal solutions.[8] The dominating form of glyoxal in these solutions is the hydrated monomer (~ 80 %, δ_H = 4.74, δ_C = 92.9 ppm, 25 °C, ref. TMS) followed by several forms of dimer. The relative intensity of the signals does not change over a temperature range from 25 to 80 °C.

In the aromatic region of the proton NMR spectra, all the compounds shown in Fig.2.2 exhibit a pair of doublets (an unresolved AA'BB' pattern) at δ_H approx. 8 ppm, characteristic for the *p*-nitrophenyl group. With the exception of the structurally rigid ammonium salt **2** (Fig.2.2) the aliphatic regions of the ^{1}H NMR spectra of the compounds measured in water contain sets of hardly distinguishable multiple signals (although the spectra are better resolved than the spectra of the corresponding 1,8-en-cyclam derivatives, see Chapter 3). In addition to these signals, in the spectra of compound **6** a wide doublet assigned to the phosphorus-attached proton ($^{1}J_{H\text{-}P}$ = 522 Hz) appears at ~ 6.9 ppm. In the ^{31}P NMR spectra of ligand **6** a corresponding doublet at δ = 26.2 ppm is present. The value of the H-P coupling constant is in range of values typical for alkyl-phosphinates R–PH(O)OH.[10]

To determine the structure of the ligand **3** in solution, several two-dimensional correlation NMR spectra have been measured (^{1}H-^{13}C gHSQC, gHMBC and ^{1}H-^{1}H COSY, NOESY). Results of the HSQC and HMBC experiments were used to assign the H-C and C-C connectivity, respectively (for the full signal assignment and the numbering scheme see Appendix II). Against the expectations, results of the NOESY measurements did not help to establish the conformation of the piperazine subunit as the exchange signals are assignable to both possible conformations.

Prior to the X-ray single crystal determination of compound **4** the NMR-based structure determination (i.e. the second acetate group location) have been undertaken. Gradient Heteronuclear Single-Quantum Correlation (gHSQC) 2D spectroscopy was used to assign the H-C connectivity and gradient Heteronuclear Multiple-Bond Correlation (gHMBC) spectroscopy was used for C-C connectivity determination. The acetate group have been localized at the nitrogen atom closer to nitrobenzyl-bearing nitrogen atom ('*cis*' to the nitrobenzyl group, '*trans*' to the second acetate group). This structural motif was later confirmed by the solid-state structure determination (see below).

2.2.3 X-ray structural studies

In order to determine the structure of the prepared compounds in the solid state, several attempts to prepare single crystals either of the ligands or their metal complexes have been done. Crystals suitable for the single crystal X-ray structure determination have been obtained from solutions of compounds **4**, **5** and the copper(II) complex of ligand **3** – [Cu(**3**)Br][PF_6]. However, the attempt to determine the solid state structure of the compound **4** failed. The crystals of this compound tended to disintegrate on the X-ray beam exposition and only the basic structural motif confirming the supposed structure of the compound had been determined.

*2.2.3.1 – Copper(II) complex of **3***

The crystal structure of the [Cu(**3**)Br][PF_6] complex exhibits a five-coordinated copper(II) (Fig.2.3). In the structure a weak coordination interaction between copper and bromine atom (Cu1–Br1A = 2.7 Å) appears . The bromine atom has been found disordered in two almost equally populated positions (relative abundance 56 : 44), the less populated position being more distant from the copper centre (3.3 Å) than the position of the weakly coordinated bromine atom. The positions of the bromine atom are probably influenced by the proximity of the N8 bound proton (N8···Br1A = 3.122 Å, N8···Br1B = 3.254 Å, but the hydrogen atom could not be localised on the difference Fourier map).

However, having in mind the low quality of the crystal used for the measurement, coordination sphere of the central copper-atom could be described as an intermediate structure between tetragonal pyramid and trigonal bipyramid. The τ-parameter describing five-coordinated geometries along the Berry rearrangement between a trigonal bipyramid and a square pyramid ($\tau = (\beta - \alpha)/60$, with $\tau = 1$ for trigonal bipyramidal and 0 for square pyramidal geometry),[11] is 0.51 (β = N1–Cu1–N8, α = N5–Cu1–N12).

The structural motif of this complex is essentially identical to a recently reported complex [Cu(**1**)Cl][$CuCl_2$][21] with the τ-parameter equal to 0.54.

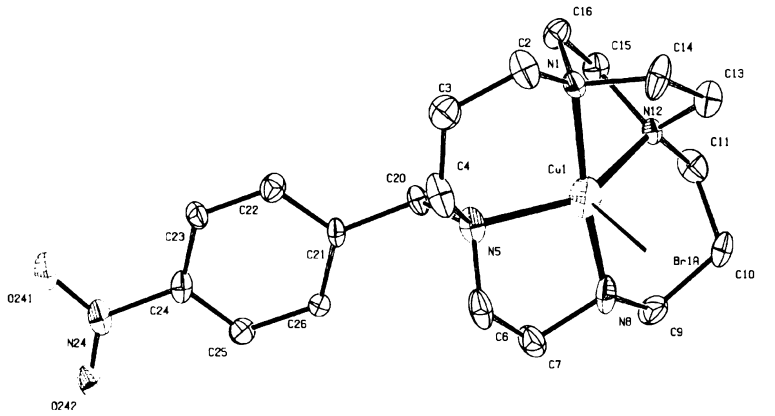

Fig.2.3 – The ORTEP view of the [Cu(**3**)Br]$^+$ ion with 30% probability thermal ellipsoids (hydrogen atoms and the bromine disorder are omitted for clarity)

Table 2.1 – Selected bond distances (Å) and bond angles (deg) in the [Cu(**3**)Br]$^+$ ion

Cu1–N12	1.996(9)	Cu1–N1	2.076(10)
Cu1–N5	2.009(10)	Cu1–N8	1.850(13)
Cu1–Br1A	2.718(8)	Cu1–Br1B	3.268
N1–Cu1–N8	173.2(4)	N8–Cu1–N5	93.5(5)
N1–Cu1–N12	76.1(4)	N8–Cu1–Br1A	83.9(4)
N1–Cu1–N5	93.2(5)	N5–Cu1–N12	142.7(4)
N1–Cu1–Br1A	96.0(4)	N12–Cu1–Br1A	116.4(3)
N8–Cu1–N12	97.8(4)	N5–Cu1–Br1A	100.0(3)

*2.2.3.2 – Crystal structure of **5**·3H$_2$O*

The ammonium salt **5** crystallizes in a zwitterionic form, with deprotonated carboxylate group and protonated N8 nitrogen atom. The piperazine ring has the 'chair' conformation (the most stable for the six-membered cyclohexane-like rings) with the lone pair of the tertiary N12 atom heading towards the inner space of the macrocyclic ring and participating in the hydrogen bonds system among the N5, N8 and N12 nitrogen atoms (H81–N12 = 2.06 Å, H81–N5 = 2.47 Å). One of the carboxylate group oxygen atoms participates in a relatively strong intermolecular hydrogen bond comprising O211# atom of the neighbouring molecule, N8 and H82 atoms (O211#···H82 = 1.94 Å). One of the central propylene carbon atoms (C13) is disordered into two positions with relative population 38 : 62. The Br$^-$ anion compensates the positive charge of the whole molecule. Furthermore, the crystal structure contains three solvate water molecules.

Table 2.2 – X-ray crystal data collection and refinement details for [Cu(**3**)Br][PF_6] and **5**·3H_2O

	[Cu(**3**)Br][PF_6]	**5**·3H_2O
Empirical formula	$C_{19}H_{31}CuN_5O_2BrF_6P$	$C_{21}H_{40}N_5O_7Br$
fw	649.91	554.49
Crystal shape	prism	prism
Color	blue-violet	yellow
Crystal system	triclinic	monoclinic
Space group	$P\bar{1}$ (No. 2)	*C*2/c (No. 15)
a (Å)	6.9960(4)	19.4788(4)
b (Å)	10.2570(8)	19.7272(4)
c (Å)	17.8780(15)	13.7214(3)
α (deg)	73.592(3)	90
β (deg)	84.539(5)	97.7160(11)
γ (deg)	80.636(4)	90
V (Å^3)	1212.60(16)	5224.88(19)
Z	2	8
ρ_{calc} (g·cm^{-3})	2.004	1.387
T (K)	293(2)	293(2)
μ (mm^{-1})	3.143	1.619
F (000)	713	2296
θ range of data collection (deg)	2.09–27.47	3.44–27.50
Index ranges, *hkl*	–8 to 7, –13 to 13, –23 to 23	–25 to 25, –25 to 25, –17 to 17
Reflections measured	5090	5978
Reflections observed [$I > 2\sigma(I)$]	3452	4839
Data, restraints, parameters	5090, 0, 327	5978, 0, 311
Goodness-of-fit on F^2	1.993	1.045
Wavelength (Å)	0.71073	0.71073
R, *R*' [$I > 2\sigma(I)$]'	0.2118, 0.1736	0.0736, 0.0590
wR, *wR*' [$I > 2\sigma(I)$]'	0.5083, 0.4929	0.1828, 0.1680
Maximum shift/esd	0.044	0.000
$\Delta\rho_{max, min}$ (e·Å^{-3})	2.415, –2.128	0.907, –0.935

$w = 1/[\sigma^2(F_o^2) + (AP)^2 + BP]$, $P = (F_o^2 + 2F_c^2)/3$; R, $R' = \Sigma|F_o - F_c|/\Sigma|F_c|$, wR, $wR' = [\Sigma w(F_o^2 - F_c^2)^2/\Sigma w(F_o^2)^2]^{1/2}$ (ref.14)

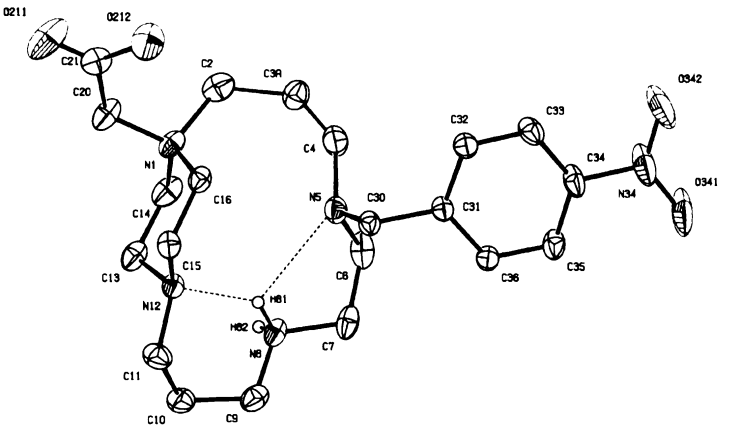

Fig.2.4 – The ORTEP view of $\mathbf{5}^{+}$ ion with 30% probability thermal ellipsoids (carbon-bound hydrogen atoms, solvate molecules and ring disorder are omitted for clarity)

Table 2.3 – Selected distances (Å) and angles (deg) in the H-bond system of $\mathbf{5}^{+}$ ion

H81···N5	2.58	N8···N5	2.91
H81···N12	2.00	N8···N12	2.80
H82···O211#	1.94	N8···O211#	2.72
N8–H81···N5	102	N8–H82···O211#	174
N8–H81···N12	148		

#: *x*, -*y*, *z*+0.5

2.2.4 Potentiometric titrations

In order to determine the acid-base properties of the newly prepared ligands and the thermodynamic stability constants of their complexes with copper(II) and zinc(II), the pH-metric titration experiments have been conducted. The resulting values of the protonation and dissociation constants of the ligands in water solution are presented in Table 2.4, whereas the stability constants of their $Cu^{(II)}$ and $Zn^{(II)}$ complexes are listed in Table 2.5.

There could be four species with different degree of protonation found in the aqueous solutions of the monosubstituted compound **3**, depending on the pH value (cf. Fig.2.5a). The fully deprotonated species could be detected and becomes predominant at pH value close to 12. The most basic nitrogen atom should be the secondary amine N8 ($pK_1 \sim 11$). The second proton is probably caught by the piperazine-ring nitrogen atom in '*trans*' position to N8 (N1; $pK_2 \sim 8$). The last two protons seem to be attached simultaneously to the ligand skeleton at the N5 and N12 atoms ($pK_3 + pK_4 \sim 3$).

Table 2.4 – Protonation and dissociation constants of the investigated compounds

	3	**6**	**1**[a]	cyclam[b]	Me_4cyclam[‡,b]
log β_1	11.35(8)	9.21(1)	---	---	---
log β_2	19.61(1)	16.54(2)	---	---	---
log β_3	---	18.13(4)	---	---	---
log β_4	22.44(3)	18.9(1)	---	---	---
pK_a (HL)	11.36	9.21	12.54	11.4	9.36
pK_a (H_2L)	8.25	7.33	9.42	10.28	9.02
pK_a (H_3L)	---	1.59	0.73	1.6	2.54
pK_a (H_4L)	2.83[#]	0.78	---	2.1	2.25

determined in 0.1 M aq. KNO_3 at 25° C ; a – data for **1** taken from ref. [17]; ‡ - 1,4,8,11-tetramethyl-1,4,8,11-tetraazacyclotetra-decane; b - data for cyclam and Me_4cyclam were taken from ref.[18]; # - pK_a(H_3L) + pK_a(H_4L)

As expected, the overall basicity of the ligand **6**, bearing an additional methylphosphinate group, is lower than the basicity of the parent compound **3**. The phosphinate compound is fully deprotonated at pH value above 9. The first proton is probably attached either to the N5 atom (bearing the *p*-nitrobenzyl group) or N8 atom (bearing the methylphosphinate). In the next step one of the piperazine ring nitrogen atoms is protonated. The lowest (the most acidic) dissociation constant correspond to protonation of the remaining nitrogen atoms and/or the methylphosphinate moiety.

The acid-base behaviour of the compound **5** was also determined. While the expected structure of the compound was **5a** (cf. Scheme 2.3), the compound exhibited an 'unusual' behaviour which was retroactively explained by its structure (determined by the 2D NMR heteronuclear correlation spectroscopy and single-crystal X-ray structure determination). Yet the bulk material contained some proton-bearing impurity (probably some amount of compound **4**, ~ 5—7 %), thus the protonation and dissociation constants values are burdened by large systematic error values. Anyway, the lowest pK value determined (1.6) can be assigned to the carboxylate proton dissociation (the pK_a value of betaine – (carboxymethyl)trimethylammonium salt – containing similar structural ammonium-cation-carboxylate-group motif, is 1.7[18]). The second dissociation constant (pK ~ 9) could be assigned to protonation of the *p*-nitrobenzyl bearing N5 atom and the highest constant (pK ~ 12) to the protonation of the secondary amino group of the macrocycle.

The acid-base behaviour of the investigated compounds can be well described as an approximation of cyclam and Me_4cyclam properties. The basicity of the secondary amino group in **3** is the same as in cyclam and is only slightly higher in **5**. The acidity of the remaining tertiary amino groups is much closer to Me_4cyclam than to cyclam. As expected, the acid-base behaviour of the compound **6** is very similar to that of Me_4cyclam (at least in the alkaline part of

the pH scale). The most acidic dissociation constant of the ligand **6** is similar to the constant obtained for aminomethylphosphinic acid.[19]

Table 2.5 – Stability constants of copper(II) and zinc(II) complexes[a]

		3		**6**		cyclam		Me_4cyclam	
Equilibrium†	*hlm*	Cu^{2+}	Zn^{2+}	Cu^{2+}	Zn^{2+}	Cu^{2+}	Zn^{2+}	Cu^{2+}	Zn^{2+}
		log β_{hlm}							
M + L ⇌ ML	011	15.50(5)	8.5(1)	14.71(3)	11.53(9)	28.1	15.2	18.3	10.4
H + L + M ⇌ HML	111	---	---	16.81(9)	16.94(5)	---	---	---	---
		pK_a							
HML ⇌ ML + H		---	---	2.10	5.41	---	---	---	---

a - determined in 0.1 M KNO_3 at 25 °C † Charges of the species are omitted for clarity; b - data for cyclam and Me_4cyclam were taken from ref.[18]

The complexation of Zn^{II} and Cu^{II} proceeded very slowly in the pH range used for the potentiometric experiments, thus the titrations involving the metal-ligand systems have been conducted using the 'out-of-cell' method (i.e. the solutions were prepared in the desired ligand-metal ratios, known amount of the base was added and the mixtures were left to equilibrate at 25 °C for 4 days).

The complexation of copper(II) and zinc(II) with ligand **3** shows usual behaviour. The ligands start to coordinate in acidic (Cu^{II}, $-\log[H^+] \sim 2$) or slightly acidic region (Zn^{II}, $-\log[H^+] \sim 5.5$) forming the expected species $[M(L)]^{2+}$ prevailing up to the strongly alkaline region (in the case of Cu^{II}). The Zn^{II}-complex decomposed at $-\log[H^+] > 9$ and some insoluble product precipitated out of the solution (probably $Zn(OH)_2$).

In the system M^{2+}-**6**, the complexation starts in strongly acidic region by formation of the $[M(HL)]^{2+}$ species, being low-abundant in the case of copper(II) (up to 20% at $-\log [H^+] \sim 2.5$) but prevailing in Zn^{2+}-**6** system (up to ~ 90% at $-\log [H^+] \sim 4.5$). On the basis of comparison of the pK_a values of the uncoordinated ligands and the complexes it seems reasonable that the first complexation step involves coordination of the phosphinate oxygen atom and at least one nitrogen atom of the macrocyclic ring (most probably the N8 atom bearing the methylphosphinate group) with the additional proton being attached to the piperazine ring N1 atom. This species transform at higher $-\log[H^+]$ values to the $[M(L)]^+$ species being the major complexes in the alkaline $-\log[H^+]$ region.

a

b

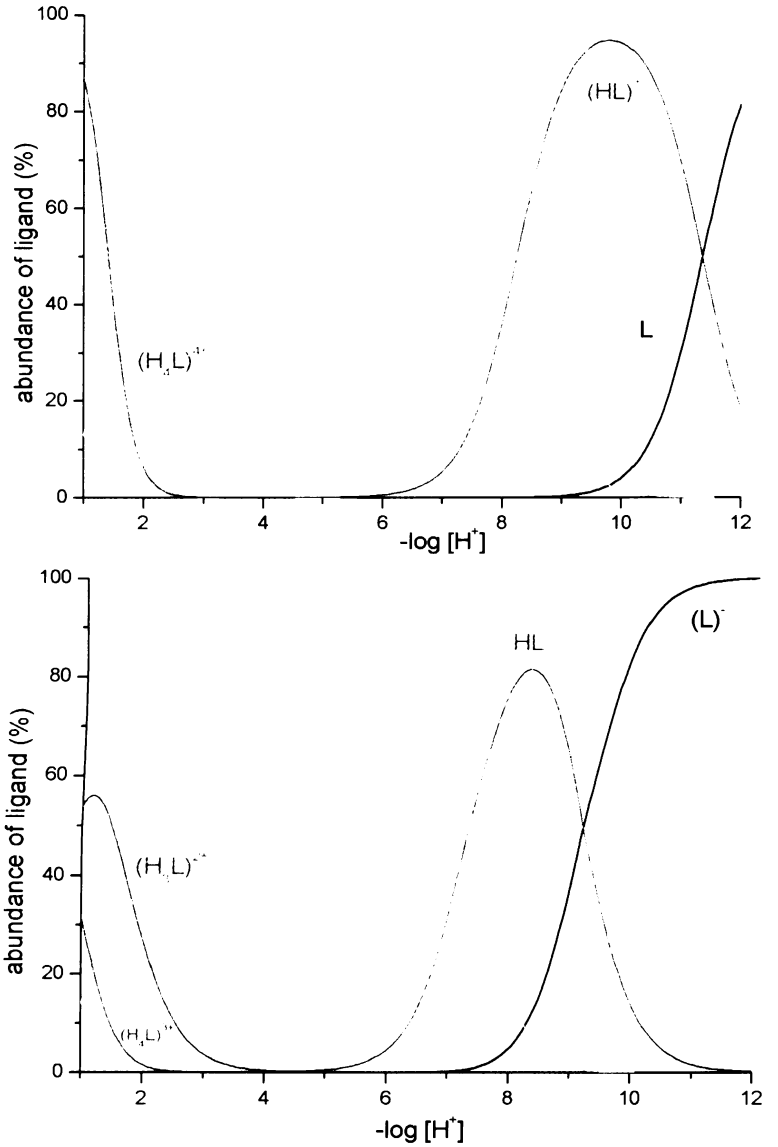

Fig.2.5 – The distribution diagrams of ligand **3** (a) and **6** (b) (0.1 M aq. KNO_3, 25 °C)

When comparing to the copper(II) and zinc(II) complexes of cyclam and Me_4cyclam, respectively, the ligands **3** and **6** form complexes with a lower thermodynamic stability. Stability of complexes of the investigated compounds is significantly lower than stability of the corresponding cyclam complexes (e.g. ~ 12 orders of magnitude for Cu(II) and ~ 7 orders of magnitude for the Zn(II) complex of **3**). On the other hand, comparison of Cu^{II} complex **3** stability constant (15.5) with the stability constant of [Cu(**1**)] (26.1, see. Ch. 1.2.4) shows the same trends in the values as in the case of Cu^{II} complexes of

Fig.2.6 – Distribution diagrams of HLM systems for Cu^{II}, Zn^{II} and ligands **3** (a, b) and **6** (c, d) (0.1 M KNO_3, 25 °C)

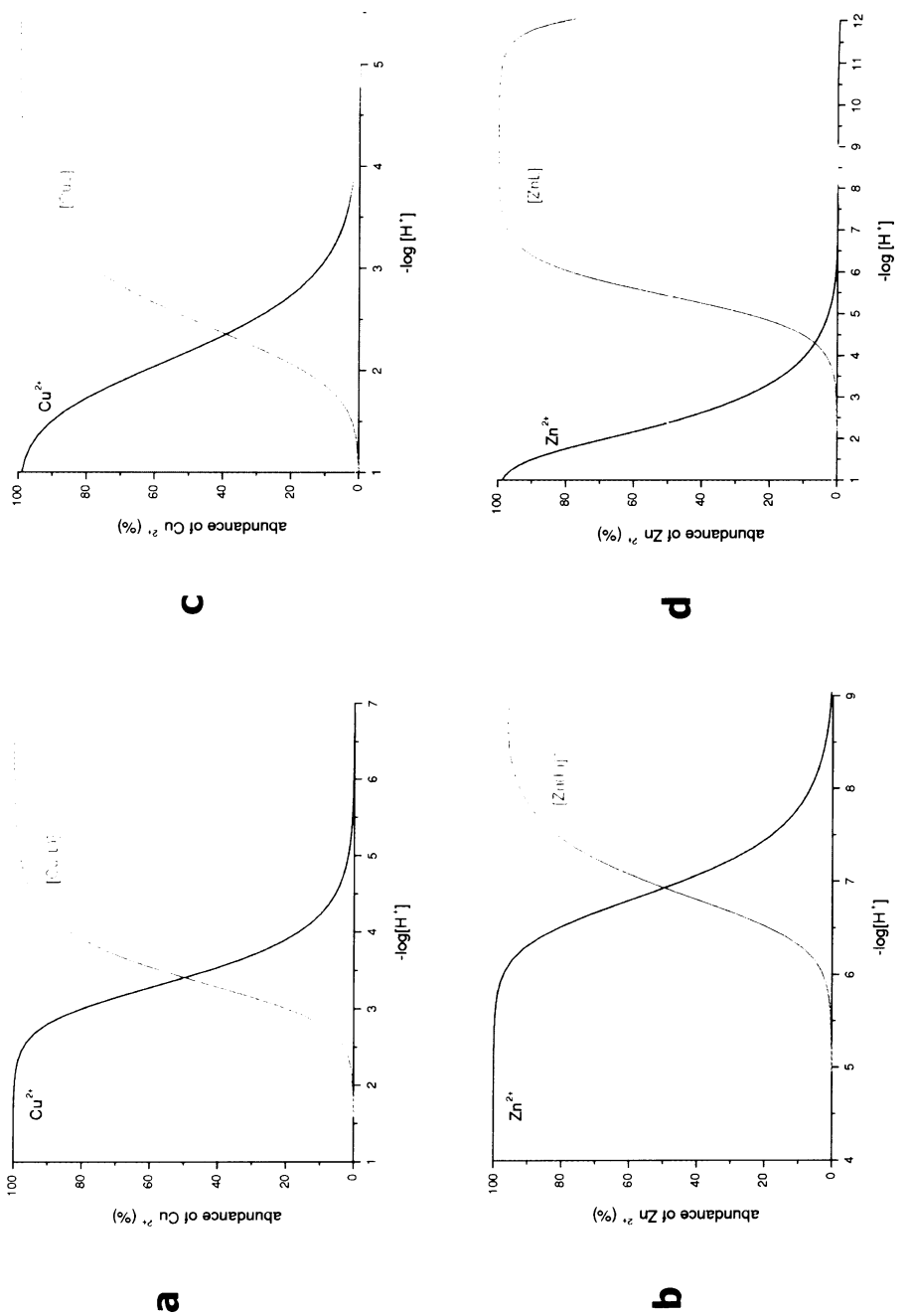

cyclam and Me_4cyclam, respectively (a difference approx. 10 orders of magnitude). The difference could be probably ascribed to lower basicity of **3** than **1** as an effect of presence of an additional substituent (*p*-nitrobenzyl group). Unfortunately, no data for a similar Zn^{II} complex are available.

The slightly higher stability observed for the Zn^{II} complex of **6** over the similar Zn^{II} complex of Me_4cyclam could be ascribed to the stabilizing effect of the hard phosphinate group present in ligand **6**.

2.3. Experimental

2.3.1 General

The analytical grade chemicals were purchased from Lachema (Czech Republic), Fluka, Sigma-Aldrich or Merck and were used as received. All the reactions were carried out under ambient atmosphere. Cyclam was prepared by slightly modified literature procedure,[12] using glyoxal hydrate trimer and Raney-Nickel. Sulfonate cation exchange resin (Dowex 50, Fluka) and an anion exchange resin (Dowex 1, Fluka) were used for column chromatography.

Elemental analyses were conducted at the Institute of Macromolecular Chemistry of Academy of Sciences of the Czech Republic (Prague). Melting points were determined using a Kofler hot-stage apparatus (Boetius) and are uncorrected. NMR spectra were recorded on a Varian Unity Inova 400 spectrometer at 400.0 MHz for ^1H, 161.9 MHz for ^{31}P and 100.6 MHz for ^{13}C nuclei with internal references TMS for $CDCl_3$ solutions and *t*-BuOH for D_2O solutions, and external reference 85% H_3PO_4. The temperature (25 °C) was controlled by a VT-regulator, containing a thermocouple calibrated using MeOH and ethylene glycol according to a reported procedure.[13] Multiplicity of the signals is indicated as follows: s – singlet, d – doublet, t – triplet, q – quintet, m – multiplet, b – broad. MS spectra were recorded on Bruker Esquire 3000 spectrometer equipped with electro-spray ion source and ion-trap detection in positive-ion mode.

2.3.1.1 Potentiometric measurements

The potentiometric titrations were carried out in a thermostated vessel at 25.0 ± 0.1 °C, at constant ionic strength $I(KNO_3)$ = 0.1 mol dm^{-3}, using a PHM 240 pH-meter, a 2 ml ABU 900 automatic piston burette and a GK 2401B combined glass electrode (Radiometer). The ligand concentration in the titration vessel was *ca.* 0.004 mol dm^{-3}. The ligand-to-metal ratio was 1 : 1 in all cases. The initial volume was *ca.* 5 ml (in the protonation constants determination experiments) or *ca.* 1 ml (in the out-of-cell experiments involving metal complexes, see below). The measurements were taken with a HNO_3 excess added to the mixture to ensure a low starting pH value. The mixtures were titrated with the stock KOH solution (~ 0.2 M) in the region of $-\log[H^+]$ = 1.6–12.0. Titrations for each system were carried out at least four

times. Each titration consisted of *ca.* 40 points (protonation constants) or 25 points (metal complexes). Inert atmosphere was provided by constant passage of argon saturated with water vapour. The metal complexation reactions were too slow to be followed by standard titrations, thus the systems were studied by the 'out-of-cell' method. Each solution was mixed separately in the test tube and an appropriate amount of the KOH solution was added to each of the test tubes to simulate the common titration. The tubes were tightly closed and left to equilibrate for four days at ambient temperature (the amount of added KOH solution and equilibration times were determined in separate preliminary experiments).

The amount of HX (X = Cl, Br) present in the ligand stock solutions was determined gravimetrically in form of AgX.

The constants with their standard deviations were calculated using the OPIUM program package.[15] The program minimises the criterion of the generalised least-squares method using the calibration function given in eq. 1:

$$E = E_0 + S \times \log[H^+] + j_1 \times [H^+] + j_2 \times K_w/[H^+] \qquad \text{eq. 1}$$

The term E_0 contains the standard potentials of the electrodes used and the contributions of inert ions to the liquid-junction potential. The term S corresponds to the Nernstian slope and the terms $j_1 \times [H^+]$ and $j_2 \times K_w/[H^+] = j_2 \times [OH^-]$ are contributions of the H^+ and OH^- ions to the liquid-junction potential. The calibration parameters were determined from titration of the standard HNO_3 with the standard KOH solution before and after every titration of the ligand/metal ion system to give calibration-titration pairs used for calculations of the stability constants. The concentration stability constants are $\beta_{hlm} = [H_hL_lM_m] / ([H]^h[L]^l[M]^m)$. The water ion product pK_w taken for calculations was 13.78.

2.3.1.2 Molecular mechanics calculations

The molecular mechanics calculations have been carried out using the HyperChem™ program package.[16] The structures with minimal total potential energy have been found using the Conformation Search module with the steepest descent search method. Each of the structures have been minimised using the MM+ force field and the Polar-Ribiere algorithm until energy gradient 0.01 kJ mol^{-1}.

2.3.1.3 Crystallography

The diffraction data were collected using a Nonius Kappa CCD diffractometer (Enraf-Nonius) at 293(2) and 150(2) K, respectively, using Mo-Kα radiation (λ = 0.71073 Å) and analysed using the HKL program package.[20] The structures were solved using direct methods and refined by full-matrix least-squares techniques (SIR92[21] and SHELXL97[14]). Scattering factors for neutral atoms were included in the SHELXL97 program. All non-hydrogen atoms were refined anisotropically. The hydrogen atoms were located in the electron density difference map; however they were fixed in theoretical or their original positions with thermal parameters U_{eq}(H) = 1.2 U_{eq}(C) or 1.3 U_{eq}(O,N), when the free refinement led to unreal bond lengths and/or extreme increase of number of refinement parameters.

2.3.2 Syntheses

*2.3.2.1 Perhydro-3a,5a,8a,10a-tetraazapyrene (**A**)*

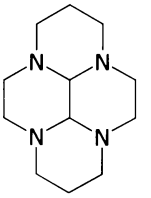

In a 50 ml flask, 1.8 g (8.6 mmol) of glyoxal trimer dihydrate were mixed with 20 ml of distilled water and heated to approximately 80 °C (until all solids dissolved). The solution was cooled to ~60 °C and mixed with 20 ml of methanol. In a separate 500 ml flask were dissolved 5 g (25 mmol) of cyclam in 200 ml of methanol and cooled using an ice-bath to ~3 °C. To this solution was added the above-prepared solution of glyoxal in a dropwise manner in ~30 minutes. The cooling bath was removed after completion of the addition and the resulting mixture was further stirred at ambient temperature for 2 h. The solvents were evaporated and 50 ml of acetonitrile were added to the mixture to precipitate the unreacted cyclam. The precipitate was filtered and the solvent evaporate do give a slightly yellow oil, which was used without any further purification. Yield 3.9 g (87 %, based on cyclam)
ESI-MS: *m/z* [M+H$^+$] = 223.2; [M+Na$^+$] = 245.2

*2.3.2.2 Perhydro-3a-(4-nitrobenzyl)-3a,5a,8a,10a-tetraazapyrenium bromide (**2**)*

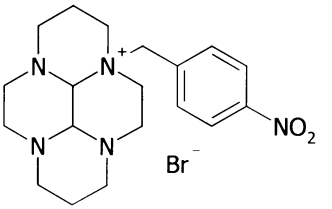

The oil prepared in the previous step was dissolved in 25 ml of anhydrous acetonitrile and 6 g (27.8 mmol) of 4-nitrobenzyl bromide were added to the solution. The mixture became cloudy after approximately 60 minutes of stirring and was further stirred for 48 hours. The resulting light yellow precipitate was filtered, washed with 10 ml of acetonitrile and 10 ml of methylene dichloride and dried in vacuo to give 9.1 g (quant., 84 % relative to cyclam) of the product in form of a yellowish powder.
m.p. = 189–190 °C; ESI-MS: *m/z* [M^+] = 358.3; ^{1}H NMR (D_2O); δ (ppm): 1.4 (bd, *J* = 13.99 Hz, 1H), 1.75 (bd, *J* = 14.33 Hz, 1H), 2.15 (qt, 2H), 2.29 (td, *J* = 13.6, 4 Hz, 2 H), 2.4–2.5 (m, 2H), 2.61 (td, *J* = 12.2, 3.2 Hz, 1H), 2.9–3.15 (m, 7H), 3.23 (td, J =13.6, 2.8 Hz, 1H), 3.31 (bd, J = 11.6 Hz, 1H), 3.45 (td, J = 13.6, 4 Hz, 1H), 3.57 (td, J = 13.6, 3.6 Hz, 1H), 3.70 (bs, 1H, C*H*), 4.19 (td, *J* = 14 , 4 Hz, 1 H), 4.32 (d, 1H, J = 1.6 Hz, C*H*), 4.81 and 5.23 (AB, *J* = 13.2 Hz, 2H, C*H*$_2$Ar), 7.75 (d, *J* = 8.8 Hz, 2H, Ar*H*), 8.27 (d, *J* = 8.8 Hz, 2H, Ar*H*); ^{13}C{^{1}H} NMR (D_2O); δ (ppm): 18.0, 18.4, 41.9, 46.6, 48.6, 51.3, 51.9, 53.3, 53.9, 60.3, 61.1, 69.5, 82.6, 124.2, 132.8, 134.6, 149.0

*2.3.2.3 5-(4-Nitrobenzyl)-1,5,8,12-tetraazabicyclo[10.2.2]hexadecane (**3**)*

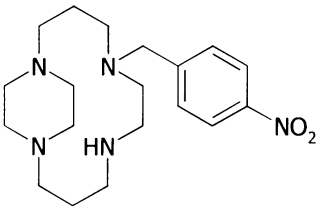

1 g (2.3 mmol) of perhydro-3a-(4-nitrobenzyl)-3a,5a,8a,10a-tetraazapyrenium bromide (**2**) was dissolved in 35 ml of EtOH/H_2O mixture (30 ml EtOH + 5 ml H_2O) at ambient temperature. To the stirred solution 0.3 g (8 mmol) of sodium borohydride ($NaBH_4$) were added and the mixture was stirred at ambient temperature overnight. The reaction was quenched by careful addition of 10 % aq. HCl (5 ml) and the solvents were evaporated. The remaining solid was dissolved in 30 ml of distilled water and the pH of the solution adjusted to ~13 by KOH. The mixture was extracted by benzene (3 x 25 ml), the organic phases were collected and dried over Na_2SO_4 and evaporated. The resulting yellow oil was used in next reaction step without further purification. Yield 0.79 g (96 %)

ESI-MS: *m/z* $[M+H]^+$ = 362.4; ^1H NMR ($CDCl_3$); δ (ppm): 1.69 (q, *J* = 4.8 Hz, 2H, -CH_2-C*H*$_2$-CH_2-), 1.76 (q, *J* = 4.8 Hz, 2H, -CH_2-C*H*$_2$-CH_2-), 2.26 (ddd, 2H), 2.53 (t, 2H), 2.55–2.70 (m, 10H), 2.90 (t, *J* = 4 Hz, 2H, -*CH*$_2$-CH_2-CH_2-), 3.02 (ddd, 2H), 3.18 (ddd, 2H), 3.71 (s, 2H, -*CH*$_1$-Ar), 7.47–7.50 and 8.16–8.20 (AA'BB', 2H each, -*Ar*); $^{13}C\{^1H\}$ NMR ($CDCl_3$); δ (ppm): 23.63, 26.10, 48.09, 48.33, 50.10, 51.22, 54.65, 54.79, 55.70, 56.95, 57.58, 123.29, 129.70, 146.89, 147.02

The yellow oil was dissolved in 49 % aq. HBr. The solution was left in a glass desiccator filled with acetone. On vapour diffusion over several days, light yellow needles of the hydrate of hydrobromide salt of **3** precipitated out of the solution. The product was filtered, washed with acetone and air-dried. Yield 1.20 g (76 %). M.p. = 182–184 °C; ESI-MS *m/z* $[M+H]^+$ = 362.4; ^1H NMR (D_2O); δ (ppm): 1.9–2.2 (bm, 4H), 2.7–3.1 (bm, 8H), 3.2–3.7 (bm, 12H), 4.1 (b, 2H), 7.48 (d, *J* = 8.8 Hz, 2H, Ar*H*), 2.20 (d, *J* = 8.8 Hz, 2H, Ar*H*); $^{13}C\{^1H\}$ NMR (D_2O); δ (ppm): 23.24, 25.78, 47.69, 48.02, 49.67, 50.92, 54.20, 54.36, 55.33, 56.57, 57.16, 122.87, 129.3, 146.53. 146.60; elem. anal. for $C_{19}H_{31}N_5O_2 \cdot 5HBr \cdot 4H_2O$: calcd. C – 27.23 %, H – 5.29 %, N – 8.36 %, found: C – 27.12 %, H – 5.34 %, N – 8.28%

*2.3.2.4 Attempted syntheses of **5a** resulting in preparation of **4***

General scheme for the carboxylate derivative preparation:

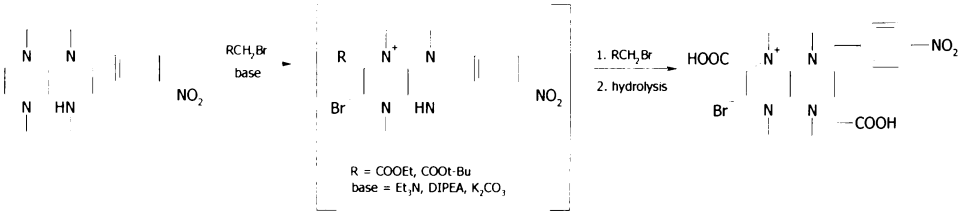

To the yellow oil prepared from 2 g of **2** as described in 2.3.2.3 dissolved in 50 ml of acetonitrile 1 equiv. of a base (0.5 g of Et_3N, 0.6 g of DIPEA or 0.7 g of K_2CO_3) was added. To the mixture 1 equiv. of the alkylating agent (0.8 g of ethyl bromoacetate or 0.9 g of *t*-butyl bromoacetate, respectively) was slowly added and the mixture was stirred overnight at ambient temperature. The resulting solution was evaporated (in the case of K_2CO_3 after filtration of the solids) and the resulting ester was hydrolysed (stirring the ethyl ester under reflux in 6 M aq. HCl or the *t*-butyl ester at ambient temperature with trifluoroacetic acid in methylene dichloride (1:1) overnight). The mixture was evaporated yielding an yellow oil, which was dissolved in ~ 5 ml of 49 % aq. HBr. On addition of several drops of distilled water the product began to crystallise within 1 min and the mixture was left for crystallisation for further 5 minutes. The resulting crystalline material was filtered, washed with cold ethanol (10 ml) and acetone (10 ml) and air-dried. Yield 4.2 g (quantitative, based on the amount of added alkylating agent) of the off-white

microcrystalline product.
M.p. = 171–172 °C; ESI-MS *m/z* $[M-H]^+$ = 477.8 (100 %), $[M-H+Na]^+$ = 500; ^{1}H NMR (D_2O); δ (ppm): 2.26 (m, 2H, -$CH_2CH_2CH_2$-), 2.4 (m, 2H, -$CH_2CH_2CH_2$-), 3.2–3.41 (m, 8H), 3.63 (t, *J* = 5.2 Hz, 2H), 3.76–3.96 (m, 6H), 4.15 (t, J = 6.8 Hz, 2H), 4.20–4.32 (m, 4H), 4.44 (s, 1H), 4.46 (s, 1H), 7.73 (d, *J* = 8.8 Hz, 2H, Ar*H*), 8.33 (d, *J* = 8.8 Hz, 2H, Ar*H*); $^{13}C\{^1H\}$ NMR (D_2O); δ (ppm): 20.04, 22.02, 45.88, 52.26, 52.74, 54.22, 55.12, 56.14, 56.32, 57.20, 58.86, 63.17, 126.61, 134.93, 139.1, 151.2, 168.2, 176.8; elem. anal. for $C_{23}H_{36}N_5O_6Br \cdot 3HBr \cdot 3H_2O$ calcd.: C – 32.30 %, H – 5.30 %, N – 8.19 %, Br – 37.37 %; found – C – 32.33 %, H – 5.28 %, N – 7.89 %, Br – 35.87 %

*2.3.2.5 1-Carboxymethyl-5-(4-nitrobenzyl)-5,8,12-triaza-1-azoniabicyclo-[10.2.2]hexadecane bromide (**5**)*

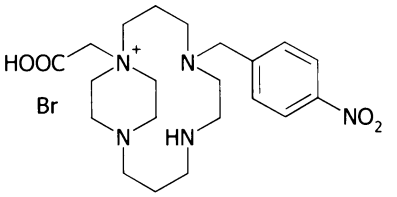

5-(4-Nitrobenzyl)-1,5,8,12-tetraazabicyclo[10.2.2]hexadecane, prepared from 2 g of **2** as described in 2.3.2.3, was dissolved in 50 ml of diethyl ether. 0.6 g (4.3 mmol, ~0.95 eq) of bromoacetic acid was dissolved in 10 ml of diethyl ether. The bromoacetic acid solution was then added in a dropwise manner with vigorous stirring to the macrocycle solution at ambient temperature. Immediately on mixing of the reagents a slightly yellow precipitate appears in the reaction mixture. After the complete addition of the alkylating agent the mixture was stirred for further 60 minutes, the liquid phase was decanted and the remaining solid was air-dried. The crude product was dissolved in EtOH / H_2O mixture (5 ml, 1 : 1) and the solution carefully covered with a large amount of acetone. After 48 hours of standing a drop of deep yellow oil separated on the bottom of the flask and some yellow crystals precipitated on the walls of the flask. The crystals were carefully separated, washed with acetone and air-dried, yielding 0.43 g of the product (19 %, ~95 % purity according to NMR measurements). 100 mg of the product have been dissolved in hot distilled water in a NMR tube. On slow cooling to room temperature yellow crystals suitable for the single-crystal X-ray analysis appeared on the walls of the tube.

The oily substance remaining after isolation of the first batch of the product was dissolved in 4 M ethanolic HBr solution. The solvents were evaporated under vacuum yielding 1.06 g of a light yellow powder (overall yield ~50 %) of purity similar to the first batch of crystals.
M.p. = 186–190 °C; ESI-MS *m/z* $[M+H]^+$ = 420.0, $[M+Na]^+$ = 442.0; ^{1}H NMR (D_2O); δ (ppm): 1.98 (q, 2H, -$CH_2CH_2CH_2$-), 2.05 (q, 2H, -$CH_2CH_2CH_2$-), 2.70–2.98 (m, 8H), 3.20–3.28 (m, 4H), 3.34 (t, *J* = 5.2 Hz, 2H), 3.39 (t, *J* = 5.3 Hz,

2H), 3.80–3.88 (bm, 4H), 3.90 (s, 2H), 4.15 (s, 2H), 7.53 (d, *J* = 8.8 Hz, 2H, Ar*H*), 8.26 (d, *J* = 8.8 Hz, 2H, Ar*H*); $^{13}C\{^{1}H\}$ (D2O); δ (ppm): 20.69, 21.67, 45.51, 49.36, 50.79, 52.07, 54.82, 55.39, 55.52, 61.96, 63.74, 123.79, 131.17, 143.59, 147.18, 168.72; Elem. anal. for $C_{21}H_{33}N_5O_4Br \cdot 3HBr \cdot 3.5H_2O$ calcd.: C – 31.29 %, H – 5.50 %, N – 8.64 %, found: C – 31.22 %, H – 5.40 %, N – 8.44 %

*2.3.2.6. [5-(4-Nitrobenzyl)-1,5,8,12-tetraazabicyclo[10.2.2]hexadec-8-yl]-methyl phosphinic acid (**6**)*

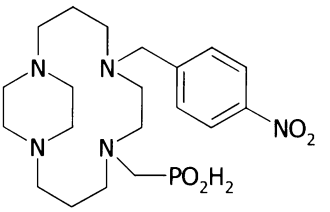

2 g of the oil prepared in 2.3.2.3 was dissolved in 10 ml of 5 M aq. HCl. To the stirred mixture 0.35 g (12 mmol) of paraformaldehyde and 1.5 g (23 mmol) of solid phosphinic acid were added and the suspension was stirred and heated to ~35 °C for 72 h. The resulting solution was evaporated in vacuo (with the water bath temperature not exceeding 40 °C), dissolved in 5 ml of distilled water and chromatographed using cation-exchanging resin (Dowex 50-4 in H^+ form, elution H_2O, 5 % aq. ammonia). The ammonia eluate was evaporated, the residue dissolved in water and re-chromatographed using an anion-exchanging resin (Dowex 1 in OH^- form, elution H_2O followed by 10 % acetic acid). The acidic eluate was evaporated, the residue dissolved in 5 ml of ethanol and 1 ml conc. aq. HCl. 100 ml of acetone was added to the solution to precipitate the product as a hydrochloride salt, which was filtered after overnight standing at ambient temperature (transformation of the amorphous precipitate to a microcrystalline powder) and dried under vacuum to yield 0.86 g of an off-white powder (64 % based on **2**).
ESI-MS *m/z* $[M+H]^+$ = 439.9; ^{1}H NMR (D_2O); δ (ppm): 2.05 (b, 2H, -CH_2-C*H*$_2$-CH_2-), 2.20 (b, 2H, -CH_2-C*H*$_2$-CH_2-), 2.60–3.85 (bm, 18H), 4.40 (s, 2H, -*CH*$_2$-Ar), 6.92 (d, *J* = 522 Hz, 1H, P-*H*), 7.70 (d, *J* = 8.8 Hz, 2H, Ar*H*), 8.20 (d, *J* = 8.8 Hz, 2H, Ar*H*); ^{31}P NMR (D_2O); δ (ppm): 26.2 (d, *J* = 522 Hz, *P*-H); Elem. anal. for $C_{20}H_{34}N_4O_5P \cdot 4HCl \cdot H_2O$ calcd.: C – 39.81 %, H – 6.68 %, N – 11.61 %, found: C – 39.73 %, H – 6.53 %, N – 11.32 %

*2.3.2.7 [5-(4-Nitrobenzyl)-1,5,8,12-tetraazabicyclo[10.2.2]hexadec-8-yl]-methyl phosphonic acid (**7**)*

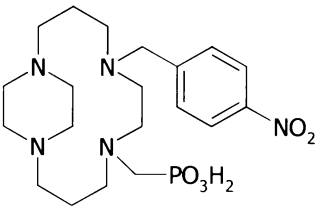

5-(4-Nitrobenzyl)-1,5,8,12-tetraazabicyclo[10.2.2]hexadecane, prepared from 2 g of **2** as described in 2.3.2.3, was dissolved in 10 ml of triethylphosphite and 0.3 g (10 mmol) of paraformaldehyde were added. The heterogeneous mixture was warmed to 50 °C and stirred at this temperature for 72 hours. The solution was cooled to ambient temperature and chromatographed using cation-exchanging resin (Dowex 50-4 in H^+-form, elution H_2O/ethanol 1 : 1, H_2O followed by conc. aq. NH_3/ethanol 1 : 1). The ammonia eluate was evaporated in vacuo to produce a diethyl ester of **7** as an yellow oil (ESI-MS *m/z* $[M+H]^+$ = 512.3). The crude ester was dissolved in 30 ml 5 M aq. HCl and refluxed for 24 h. The solvent was evaporated, the residue dissolved in 2 ml of 49 % aq. HBr and precipitated by addition of 100 ml of acetone. On standing for 48 h the amorphous solid became more compact and was filtered, washed with 20 ml of acetone and dried under vacuum to yield 0.31 g (12 % of expected amount based on **2**) as a light yellow powder.
M.p. = 179–180 °C; ESI-MS *m/z* $[M+H]^+$ = 455.8; ^{1}H NMR (D_2O); δ (ppm): 2.1–2.45 (m, 4H, -CH_2-C*H*$_2$-CH_2-), 2.75–4.15 (bm, 18H), 4.52 (s, 2H, -C*H2*-Ar), 7.83 (d, J = 8.8 Hz, 2H, Ar*H*), 8.36 (d, J = 8.8 Hz, 2H, Ar*H*); ^{31}P NMR (D_2O); δ (ppm): 22.62 (s, pH ~ 1), 18.69 (s, pH ~ 13, NaOH); ^{13}C{^{1}H} NMR (D_2O, pH ~ 13); δ (ppm): 21.7, 21.9, 44.0, 44.4, 47.5, 47.9, 50.1, 50.4, 51.1, 51.9, 53.8, 58.0, 123.5, 130.9, 145.4, 146.9; Elem. anal. for $C_{20}H_{33}N_5O_4P{\cdot}4HBr{\cdot}2H_2O$ calcd.: C – 30.10 %, H – 5.18 %, N – 8.77 %; found: C – 30.23 %, H – 5.19 %; N – 8.45 %

*2.3.2.8 Preparation of [Cu(**3**)Br][PF_6]*

100 mg (0.1 mmol) of **3**·5HBr·4H_2O were dissolved in 1 ml of distilled water. 21 mg (0.1 mmol) of $CuCl_2{\cdot}2H_2O$ were dissolved in another 1 ml of water and this solution was added to the solution of ligand **3**. The violet-blue solution was refluxed for 10 minutes and 1 ml of ethanolic solution of 20 mg of NH_4PF_6 was added. The final solution was concentrated under reduced pressure to precipitate the complex, which was filtered, washed by 1 ml of H_2O and 1 ml of ethanol and air dried to yield 54 mg (70 %) of deep violet powder. This product was recrystallised from 1 ml of acetonitrile to form blue-violet single crystals suitable for X-ray structure determination.

2.4. Conclusions

Synthesis of a series of new compounds built on 1,4-en-cyclam skeleton is reported. During the synthetic procedure an unexpected alkylation pathway of the mono-*p*-nitrobenzyl-substituted derivative was observed. The protonation constants of the ligands together with the thermodynamic stability constants of their copper(II) and zinc(II) complexes are surprisingly lower than expected for the constrained azamacrocycles. Formation of the metal complexes is relatively slow at room temperature, thus the pH-metric experiment cannot be followed by common procedure but using the out-of-cell method; however these complexes should be of use for complexation of copper radioisotopes with life-time in order of hours (^{64}Cu and ^{67}Cu). The thermodynamic stability constants of the Cu^{II} complex of **3** are approx. 10 orders of magnitude lower than the constants of the similar complex of ligand **1** (15.5 vs. 26.1). The difference is in good agreement with the constants observed for copper(II) complexes of cyclam and Me_4cyclam (28.1 vs. 18.3).

The solid state structure of the [Cu(**3**)Br][PF_6] complex have also been determined; the copper central atom is surrounded by the macrocycle and the bromine atom forming a coordination sphere which is an intermediate between trigonal-bipyramid and square-pyramid (τ-parameter equal to 0.51).

>-----<

References:

[1] T. J. Hubin, *Coord. Chem. Rev.*, **2003**, *241*, 27
[2] J. Springborg, *Dalton Trans.*, **2003**, 1653
[3] K. P. Wainwright, *Inorg. Chem.*, **1980**, *19*, 1396
[4] M. Boiocchi, M. Bonizzoni, L. Fabbrizzi, F. Foti, M. Licchelli, A. Poggi, A. Taglietti, M. Zema, *Chem. Eur. J.*, **2004**, *10*, 3209
[5] R.A. Kolinski, *Polish. J. Chem.*, **1995**, *69*, 1039
[6] S. J. Archibald, E. A. Lewis, T. J. Hubin, *PCT WO-2005/121109 A2,* December 22nd, **2005**
[7] E. H. Wong, G. R. Weisman, D. C. Hill, D. P. Reed, M. E. Rogers, J. S. Condon, M. A. Fagan, J. C. Calabrese, K.-Ch. Lam, I. A. Guzei, A. L. Rheingold, *J. Am. Chem. Soc.*, **2000**, *122*, 10561
[8] E. B. Whipple, *J. Am. Chem. Soc.*, **1970**, *92*, 7183
[9] F. Chastrette, C. Bracoud, M. Chastrette, G. Mattioda, Y. Christidis, *Bull. Soc. Chim. France*, **1983**, *1-2*, II-33
[10] J. C. Tebby, *CRC Handbook of Phosphorus-31 Nuclear Magnetic Resonance Data*
[11] A. Addison, T. N. Rao, J. Reedjik, J. van Rijn, G. C. Verschoor, *J. Chem. Soc., Dalton Trans.*, **1984**, 1349
[12] E. K. Barefield, F. Wagner, K. D. Hodges, *Inorg. Chem.*, **1976**, *15*, 1370;

I. Meunier, A. K. Mishra, B. Hanquet, P. Cocolios, R. Guilard, *Can. J. Chem.*, **1995**, *73*, 685
[13] J. Bornais, S. Brownstein, *J. Magn. Reson.*, **1978**, *29*, 207
[14] G. M. Sheldrick, SHELXL97. *Program for Crystal Structure Refinement from Diffraction Data.* University of Göttingen, Göttingen, 1997
[15] a) M. Kývala and I. Lukeš, *Chemometrics '95*, Abstract book p. 63, Pardubice, Czech Republic, 1995; full version of *OPIUM* software package is available (free of charge) on http://www.natur.cuni.cz/~kyvala/opium.html; b) M. Kývala, P. Lubal and I. Lukeš, *IX. Spanish-Italian, and Mediterranean Congress on Thermodynamics of Metal Complexes (SIMEC 98)*, Girona, Spain, 1998
[16] HyperChem™, Hypercube, Inc., 1115 NW 4th Street, Gainesville, Florida, 32601, U.S.A.
[17] T.M. Jones-Wilson, K. A. Deal, C. J. Anderson, D. W. McCarthy, Z. Kovacs, R. J. Motekaitis, A. D. Sherry, A. E. Martell, M. J. Welch, *Nucl. Med. Biol.*, **1998**, *25*, 523
[18] R. M. Smith, A. E. Martell, *NIST Critically Selected Stability Constants of Metal Complexes Database, ver. 7.0*, **2003**
[19] J. Rohovec, I. Lukeš, P. Vojtíšek, I. Císařová, P. Hermann, *J. Chem. Soc. Dalton Trans.*, **1996**, *13*, 2685
[20] Z. Otwinowski, W. Minor, *HKL Denzo and Scalepack Program Package by Nonius BV*, Delft, **1997**; Z. Otwinowski, W. Minor, *Methods Enzymol.*, **1997**, *276*, 307
[21] A. Altomare, M. C. Burla, M. Camalli, G. L. Cascarano, C. Giacovazzo, A. Guagliardi, A. G. G. Moliterni, G. Polidori, R. Spagna, *J. Appl. Crystallogr.*, **1999**, *32*, 115
[22] A. Khan, J. D. Silversides, L. Madden, J. Greenman, S. J. Archibald, *Chem. Commun.*, **2007**, 416; J. D. Silversides, C. C. Allan, S. J. Archibald, *Dalton Trans.*, **2007**, 971

>-----<

Chapter Three

1,8-ethylene bridged (cross-bridged) cyclam derivatives: Syntheses, crystal structures and solution studies

Abstract

Synthetic procedures leading to preparation of novel, symmetrically and unsymmetrically substituted derivatives of 1,4,8,11-tetraazabicyclo[6.6.2]hexadecane (1,8-en-bridged, cross-bridged cyclam) have been developed. The compounds were characterised and studied by NMR and MS spectral methods, the solid-state structures of several ligands and their copper(II) complexes were determined by the single-crystal X-ray study.

3.1 Introduction

Tetraazamacrocycles bridged by two-carbon chain across non-adjacent nitrogen atoms are of growing importance due to the exceptional kinetic inertness of their metal complexes.[1] These complexes are potentially useful for homogenous catalysis,[2] or in radiopharmaceutical chemistry.[3] Copper(II) complexes of various derivatives of cross-bridged cyclam (1,8-en-cyclam) are more than suitable alternative to complexes of conventional cyclam-based ligands found in radiochemical clinical daily use.[4] Sterical shape of the ligands make them well suitable for formation of kinetically inert metal complexes. On the other hand, these compounds exhibit a proton-sponge behaviour,[5] which makes the incorporation of the metal into the ligand cavity very difficult.

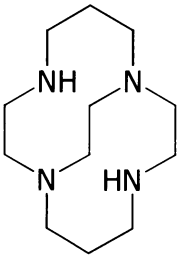

8

Fig.3.1 – Structure of 1,4,8,11-tetraazabicyclo[6.6.2]hexadecane (1,8-en-cyclam)

The majority of the ligands built-up on the 1,8-en-cyclam skeleton (Fig.3.1) contains (in addition to the ethylene bridge) two other substituents. These substituents are usually of the same kind – alkyl groups, arylalkyl or acetate (in form of an ester, amide or free acid) groups.[5] For the purpose of either radiolabelling or fluorescence labelling of biomolecules the bifunctional ligands would be more suitable. The functional group suitable for the immediate conjugation with a biomolecule or for a conjugation after a simple modification step can be connected to the azacycle skeleton either at the carbon or nitrogen atoms of the ring.[6] The benefit of the introduction of such moiety to carbon atom is overall higher stability of these ligands (C–C bond vs. C–N bond) and their possible higher hapticity (e.g. in the case of *p*-nitrobenzyl as a conjugating group precursor) for a metal ion coordination. A disadvantage are relatively more demanding synthetic procedures leading to the final products. On the other hand, introduction of the conjugating group to the nitrogen atom of the ring may lower the maximum hapticity of the ligand (which, especially in case of copper(II), may not significantly worsen the stability of the complex, see Appendix III) but the synthetic procedure leading to the the ligand is significantly easier.

3.2 Results and discussion

3.2.1 Synthesis

Synthesis of the amine **8** is well described in the literature.[7] For the unsymmetrical substitution of the starting amine, *p*-nitrobenzyl bromide have been chosen as a suitable agent. Alkylation of one of the secondary amine nitrogen atoms in non-polar solvent produces selectively monosubstituted amine **9** in high yield (Scheme 3.1).

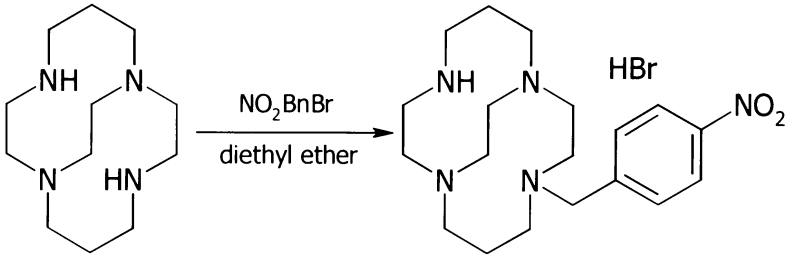

Scheme 3.1 – Selective introduction of one nitrobenzyl group

Presence of only a trace amount of more polar solvent (e.g. chloroform from the starting amine **8** extraction step) in the reaction mixture results in the second alkylation step producing the bis(*p*-nitrobenzyl) derivative **10**. This side reaction is suppressed if the amine **8** extraction is done using benzene as the organic phase.

The monoalkylated amine **9** can be further modified either by alkylation with a another alkylating agent in a polar solvent (e.g. acetonitrile) in presence of a base (e.g. K_2CO_3) or by a Mannich-type reaction involving the amine, paraformaldehyde and phosphinic acid. The hydroxymethylphosphinate side-products were present as a result of the reaction between the P–H moiety and paraformaldehyde present in the reaction mixture in an excess (Scheme 2.2). The amount of this side-product was significantly lowered by decreasing the reaction temperature from the original range 45–50 °C to temperature lower than or equal to 30 °C. At these conditions this side product was not further detected.

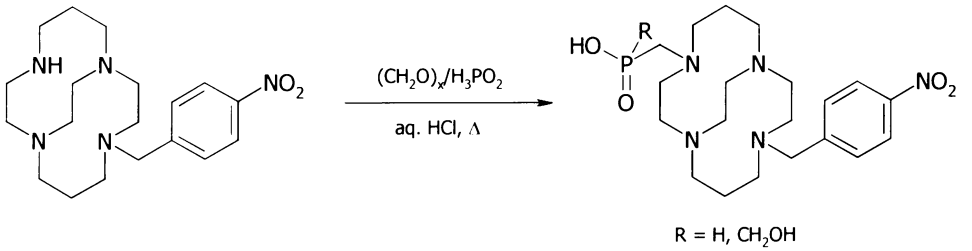

R = H, CH_2OH

Scheme 2.2 – Mannich reaction between **9** and $(CH_2O)_x/H_3PO_2$

The attempts to prepare an analogous methylphosphonate derivative similarly to preparation of **7** in Chapter 2 ($P(OEt)_3$, paraformaldehyde, heating 3 d at 70 °C) failed, particularly due to the limited solubility of **9** (either as hydrobromide or hydroxide) in triethylphosphite. Similar reaction of **8** also failed, showing that the solubility might have been not the only reason why this reaction does not proceed with this group of compounds.

Similar reaction of amine **8** with paraformaldehyde and phosphinic acid in acidic aqueous media resulted (depending on the reaction temperature) to formation of mono- and/or bis(phosphinomethyl) derivatives **13** and **14** that can be separated using the ion exchange resins.

Alkylation of **9** with ethyl bromacetate in presence of a base yielded the appropriate alkyl acetate **11a**. Acid hydrolysis of this ester in aq. hydrochloric acid yields the acetic acid derivative **11**.

The newly prepared and characterised compounds are shown in Fig. 3.2.

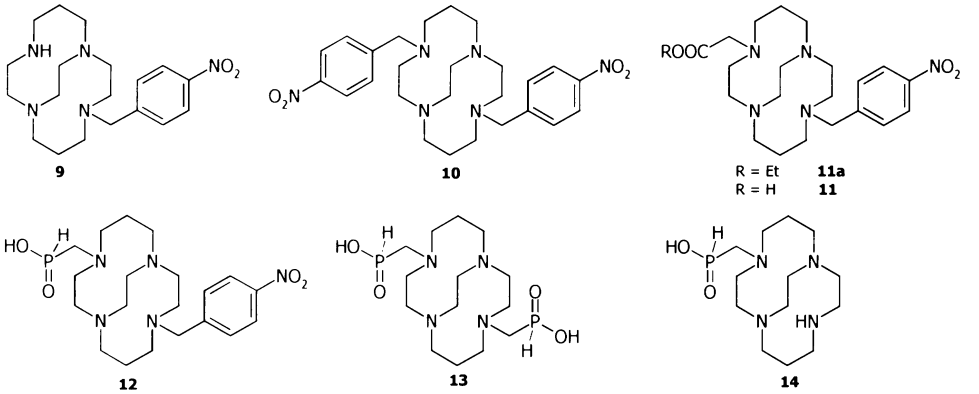

Fig.3.2 – Overview of compounds prepared in this work

3.2.2 NMR spectroscopy

The overall shape of the proton NMR spectra of the *p*-nitrobenzyl-substituted compounds mentioned above is very similar to their 1,4-en-cyclam analogues. In the aromatic region of the spectra a AA'BB' pattern characteristic for a *p*-substituted aromatic ring appears. In the case of compound **9**, two signals, that can be assigned to the secondary amine proton (δ = 11.26 ppm) and to the proton kept inside the cavity of the molecule (δ = 9.37 ppm; both shift values measured in $CDCl_3$) are detectable. A similar signal (with δ ~9 ppm was observed in the spectrum of compound **11a**).

With the exception of the acetate **11** (where the signals are hidden among many others), the spectra of other *p*-nitrobenzyl-substituted ligands contain an easily distinguishable AB spin system of the *p*-nitrobenzyl methylene group protons, with J_{AB} ~14 Hz. These AB signals are the only signals that can be clearly identified. Signals of the protons attached to the macrocyclic ring of the compounds are cumulated in several hardly resolved multiplets.

The carbon NMR spectra of these compounds contain the number of signals expected for such asymmetrical molecules (17 in **9** to 19 or 21 in **11** or **11a**, respectively).

On the other hand, the aliphatic regions of the proton spectra of the more symmetric compounds **10** and **13** are much better resolved, forming several clearly separated multiplets. In addition to these signals an P-H splitting (with $^{1}J_{P\text{-}H} \sim 550$) can be observed in the spectra of **13** and **14**.

3.2.3 X-ray structural studies

Several attempts to prepare and isolate single crystals of the investigated compounds (and their copper(II) complexes) have been successfully made, thus the solid-state structures are presented for the 4,11-dibenzyl-1,4,8,11-tetraazabicyclo[6.6.2]hexadecane intermediate **8a**, amine **9** bis(methylenephosphinic acid) **13** and Cu^{II} complexes [Cu(**9**)Cl]Cl and [Cu(**13a**)] (where **13a** represents the 1,4,8,11-tetraazabicyclo[6.6.2]-hexadecane-4,11-bis(methylphosphonic acid), Fig. 3).

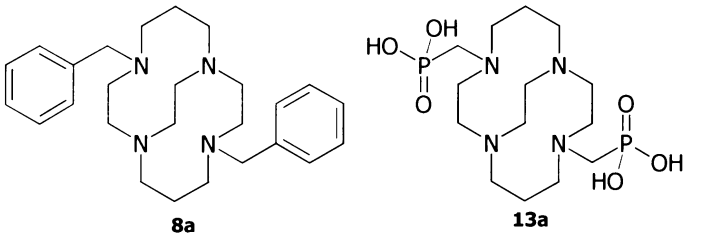

8a **13a**

Fig.3.3 – Structure of compound **8a** and ligand **13a**

*3.2.3.1 Crystal structure of the intermediate **8a***

Although the synthesis of compound **8a** was reported for the first time 10 years ago and many transition metal complexes of this ligand have been reported,[5],[7],[8] its solid-state structure have not been determined yet.

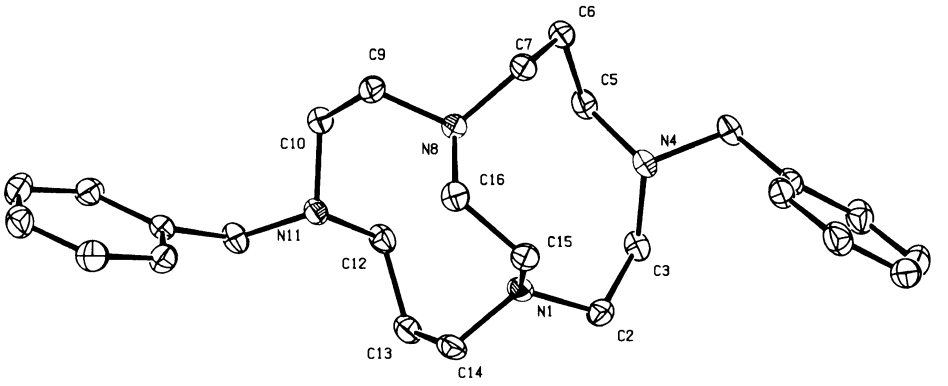

Fig.3.4 – The ORTEP view of compound **8a** with 30 % probability thermal ellipsoids (hydrogen atoms are omitted for clarity)

The compound crystallises with two almost identical (Fig. 3.5) molecules belonging to the asymmetric unit. The 1,8-en-cyclam unit is folded to form a cavity with N1–N8 distance ~2.9 Å and N4–N11 distance ~5.3 Å. None of the nitrogen atoms of the macrocycle is protonated (no proton was localized in the electron density difference map and no counterion have been found). The electron pairs at N4 and N11 atoms are headed outwards the cavity. Crystal, data collection, and refinement parameters of the X-ray diffraction study of this compound are given in Table 3.1.

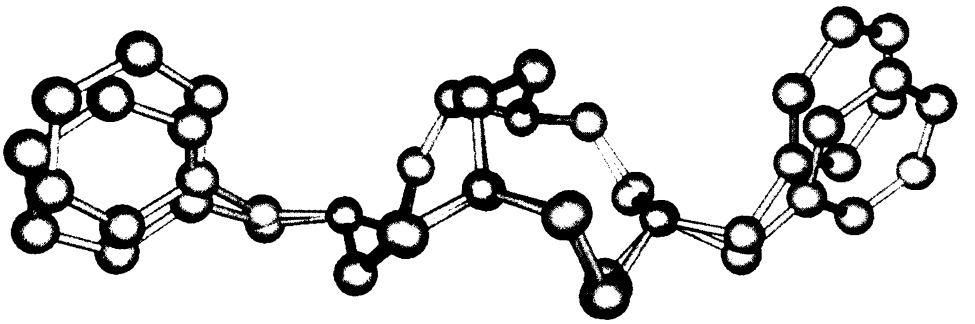

Fig.3.5 – View of an overlap of two independent molecules found in the structure of **8a**

3.2.3.2 Crystal structure of ***9***·*HBr*·*$(CH_3)_2CO$*

This ligand crystallises from the acetone solutions in form of hydrobromide salt as acetone solvate (see Ch. 3.3.2.3). The additional proton is bound to the most basic secondary amine nitrogen atom (Fig. 3.6). This proton is involved in an intramolecular hydrogen bond system further comprising N1, N4 and N8 atoms with the structural parameters given in Table 3.4. The overall structural motif is slightly different from that of the dibenzyl intermediate **8a**, which crystallizes in completely deprotonated form. Due to the presence of an additional proton in the structure of the compound **9**, the electron lone-pairs of the tertiary amine nitrogen atoms are headed towards the inner space of the bowl formed by the macrocycle. The cross-space distances between N1–N8 and N4–N11 atoms are ~2.8 and ~3.1 Å, respectively, i.e. the cavity is more compact than in the case of the above-mentioned intermediate **8a**.

The crystal, data collection, and refinement parameters of the X-ray diffraction study of compound **9**·HBr·Me_2CO are given in Table 3.2.

Table 3.1 – X-ray crystal data collection and refinement details for the intermediate **8a**

	8a
Empirical formula	$C_{26}H_{38}N_4$
fw	406.60
Crystal shape	prism
Color	colorless
Crystal system	triclinic
Space group	$P\bar{1}$ (No. 2)
a (Å)	11.8352(3)
b (Å)	12.1285(2)
c (Å)	17.4415(4)
α (deg)	77.6745(12)
β (deg)	89.8743(9)
γ (deg)	75.0877(11)
V (Å^3)	2359.84(9)
Z	4
ρ_{calc} (g·cm^{-3})	1.144
T (K)	150(2)
μ (mm^{-1})	0.068
F (000)	888
θ range of data collection (deg)	1.91–27.57
Index ranges, *hkl*	–15 to 15, –15 to 15, –22 to 22
Reflections measured	10840
Reflections observed [$I > 2\sigma(I)$]	7954
Data, restraints, parameters	10840, 0, 845
Goodness-of-fit on F^2	1.046
Wavelength (Å)	0.71073
R, *R'* [$I > 2\sigma(I)$]†	0.0671, 0.0431
wR, *wR'* [$I > 2\sigma(I)$]†	0.1088, 0.0967
Maximum shift/esd	0.001
$\Delta\rho_{max,\ min}$ (e·Å^{-3})	0.164, –0.184

$w = 1/[\sigma^2(F_o^2) + (AP)^2 + BP]$, $P = (F_o^2 + 2F_c^2)/3$; R, $R' = \Sigma|F_o - F_c|/\Sigma|F_c|$, wR, $wR' = [\Sigma w(F_o^2 - F_c^2)^2/\Sigma w(F_o^2)^2]^{1/2}$ (ref. 9)

Table 3.2 – X-ray crystal data collection and refinement details for compound **9**·HBr·Me_2CO

	9·HBr·Me_2CO
Empirical formula	$C_{22}H_{38}N_5O_3Br$
fw	500.48
Crystal shape	prism
Color	pale yellow
Crystal system	monoclinic
Space group	$P2_1/c$ (No. 14)
a (Å)	13.9700(2)
b (Å)	9.9980(1)
c (Å)	18.1380(3)
α (deg)	90
β (deg)	104.125(1)
γ (deg)	90
V (Å^3)	2456.78(6)
Z	4
ρ_{calc} (g·cm^{-3})	1.353
T (K)	150(2)
μ (mm^{-1})	1.705
F (000)	1056
θ range of data collection (deg)	2.93–27.47
Index ranges, *hkl*	−18 to 18, −12 to 12, −23 to 22
Reflections measured	5599
Reflections observed [$I > 2\sigma(I)$]	4818
Data, restraints, parameters	5599, 0, 432
Goodness-of-fit on F^2	1.051
Wavelength (Å)	0.71073
R, *R'* [$I > 2\sigma(I)$]*	0.0382, 0.0300
wR, *wR'* [$I > 2\sigma(I)$]*	0.0757, 0.0728
Maximum shift/esd	0.004
$\Delta\rho_{max,\ min}$ (e·Å^{-3})	0.370, −0.595

$w = 1/[\sigma^2(F_o^2) + (AP)^2 + BP]$, $P = (F_o^2 + 2F_c^2)/3$; R, $R' = \Sigma|F_o - F_c|/\Sigma|F_c|$, wR, $wR' = [\Sigma w(F_o^2 - F_c^2)^2/\Sigma w(F_o^2)^2]^{1/2}$ (ref.9)

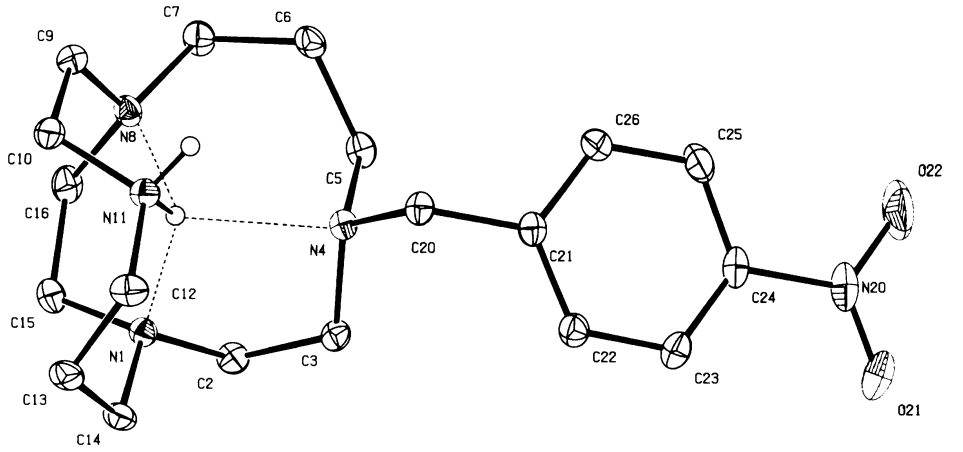

Fig.3.6 – ORTEP view of the H**9**$^+$ cation with the intramolecular hydrogen bonds (30 % probability thermal ellipsoids; carbon-bound hydrogen atoms are omitted for clarity)

Table 3.3 – Distances (Å) and angles (deg) in the system of intramolecular hydrogen bonds in H**9**$^+$

H112···N1	2.01	N1···N11	2.73
H112···N4	2.38	N4···N11	3.14
H112···N8	2.29	N8···N11	2.78
N11–H112···N1	133	N11–H112···N4	139
N11–H112···N8	112		

*3.2.3.3 Crystal structure of **13**·5H$_2$O*

The diphosphinate-substituted 1,8-en-cyclam crystallises in form of a pentahydrate. The N4 and N11 atoms bearing the methylphosphinate groups are both protonated. These protons are enclosed inside the macrocyclic cavity and participate in the intramolecular hydrogen bonds system involving all the nitrogen atoms of the macrocycle and one oxygen atom of each of the methylphosphinate groups. All the remaining phosphinate oxygen atoms participate in the intermolecular system of hydrogen bonds together with the water molecules of crystallisation. The hydrogen bonds parameters (lengths, angles) are listed in Table 3.4. The P–O distances in the methylphosphinate groups suggest delocalization of the negative charge over both oxygen atoms of each HPO_2^- moiety (P1–O11 = 1.490 Å, P1–O12 = 1.505 Å, P2–O21 = 1.492 Å and P2–O22 = 1.508 Å, respectively). The crystal, data collection, and refinement parameters of the X-ray diffraction study of compound **13**·5H$_2$O are given in Table 3.5.

Table 3.4 – Distances (Å) and angles (deg) in the system of intramolecular hydrogen bonds in **13**·5H_2O

H4···N8	2.04	N4···N8	2.80
H4···N1	2.60	N4···N1	3.05
H11···N1	2.02	N11···N1	2.78
H11···N8	2.64	N11···N8	3.05
H4···O11	2.57	N4···O11	2.93
H11···O21	2.67	N11···O21	3.01
N4–H4···N8	146	N4–H4···N1	113
N11–H11···N1	147	N11–H11···N8	111
N11–H11···O21	105		

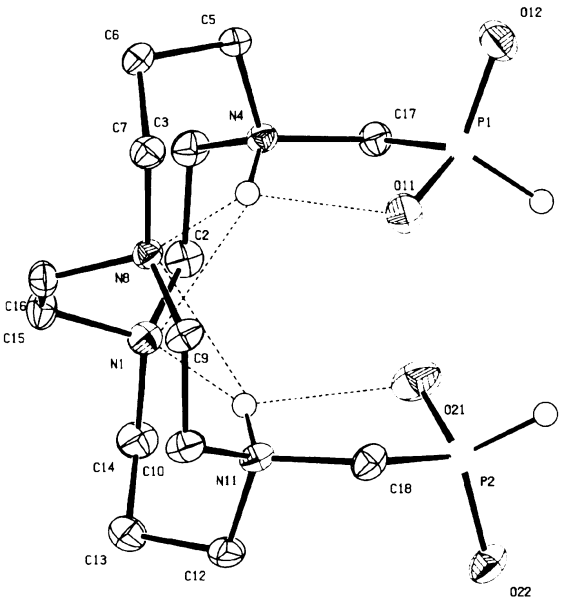

Fig.3.7 – ORTEP view of molecule of **3** with 50% probability thermal ellipsoids (carbon-bound hydrogen atoms and solvate molecules are omitted for clarity)

Table 3.5 – X-ray crystal data collection and refinement details for compound **13**·5H_2O

	13·5H_2O
Empirical formula	$C_{14}H_{42}N_4O_9P_2$
fw	472.46
Crystal shape	plate
Color	colorless
Crystal system	triclinic
Space group	$P\bar{1}$ (No. 2)
a (Å)	8.2540(1)
b (Å)	12.0390(3)
c (Å)	12.3130(3)
α (deg)	104.753(1)
β (deg)	91.0000(13)
γ (deg)	107.1200(13)
V (Å^3)	1125.11(4)
Z	2
ρ_{calc} (g·cm^{-3})	1.395
T (K)	150(2)
μ (mm^{-1})	0.245
F (000)	512
θ range of data collection (deg)	1.72–27.45
Index ranges, *hkl*	−10 to 10, −15 to 15, −15 to 15
Reflections measured	5107
Reflections observed [$I > 2\sigma(I)$]	4545
Data, restraints, parameters	5107, 0, 430
Goodness-of-fit on F^2	1.035
Wavelength (Å)	0.71073
RI R' [$I > 2\sigma(I)$]'	0.0359, 0.0309
wRI wR' [$I \geq 2\sigma(I)$]'	0.0859, 0.0821
Maximum shift/esd	0.000
$\Delta\rho_{max, min}$ (e·Å^{-3})	0.326, −0.335

$w = 1/[\sigma^2(F_o^2) + (AP)^2 + BP]$, $P = (F_o^2 + 2F_c^2)/3$; R, $R' = \Sigma|F_o - F_c|/\Sigma|F_c|$, wR, $wR' = [\Sigma w(F_o^2 - F_c^2)^2/\Sigma w(F_o^2)^2]^{1/2}$ (ref. 9)

*3.2.3.4 Crystal structure of [Cu(**9**)Cl]Cl·2H_2O*

The structural motif in the crystal structure of [Cu(**9**)Cl]Cl·2H_2O is closely related to that reported for the similar complex [Cu(**8a**)Cl]Cl·H_2O.[5] The copper central atom coordination sphere evokes an octahedron with one missing vertex. The sixth coordination site is blocked by presence of the *p*-

nitrobenzyl group and, similarly to the complex of compound **8a**, an agostic interaction between H22 atom of the phenyl ring and the copper atom can be found (H22···Cu1 = 2.715 Å). When described as a penta-coordinate complex, the copper(II) coordination sphere may be best described as square-pyramidal (the τ parameter = 0.18),[10] with the N8 atom in the apical position. The crystal structure of the complex is shown in Fig.3.8, selected bond distances and angles are listed in Table 3.6 and the crystal, data collection and refinement details are given in Table 3.7.

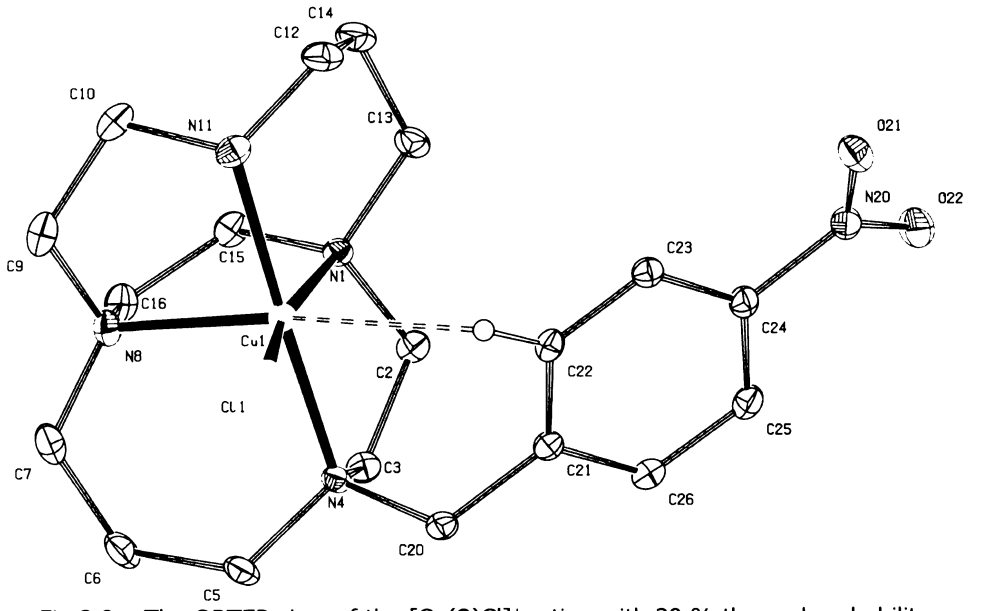

Fig.3.8 – The ORTEP view of the [Cu(**9**)Cl]$^+$ cation with 30 % thermal probability ellipsoids (hydrogen atoms (except H22) and solvate molecules omitted for clarity)

Table 3.6 – Selected bond distances (Å) and angles (deg) in the [Cu(**5**)Cl]$^+$ ion

Cu1–N1	2.0636(15)	Cu1–N4	2.0475(15)
Cu1–N8	2.1592(16)	Cu1–N11	2.0398(16)
Cu1–Cl1	2.3035(5)		
N1–Cu1–Cl1	166.32(4)	N4–Cu1–N11	177.30(6)
N1–Cu1–N4	87.05(6)	N1–Cu1–N8	87.11(6)
N1–Cu1–N11	90.41(6)	N4–Cu1–N8	95.84(6)
N8–Cu1–N11	84.94(7)	N4–Cu1–Cl1	93.27(4)
N8–Cu1–Cl1	93.27(4)	N11–Cu1–Cl1	88.98(5)

Table 3.7 – X-ray crystal data collection and refinement details for complex [Cu(**9**)Cl]Cl·2H_2O

	[Cu(**9**)Cl]Cl·2H_2O
Empirical formula	$C_{19}H_{34}N_5O_4Cl_2Cu$
fw	530.95
Crystal shape	prism
Color	deep blue
Crystal system	triclinic
Space group	$P\bar{1}$ (No. 2)
a (Å)	8.8769(2)
b (Å)	9.7692(3)
c (Å)	14.8750(4)
α (deg)	85.0128(12)
β (deg)	88.7051(16)
γ (deg)	64.0158(13)
V (Å^3)	1155.00(5)
Z	2
ρ_{calc} (g·cm^{-3})	1.527
T (K)	150(2)
μ (mm^{-1})	1.213
F (000)	556
θ range of data collection (deg)	1.37–27.54
Index ranges, *hkl*	−11 to 10, −12 to 12, −19 to 19
Reflections measured	5292
Reflections observed [$I > 2\sigma(I)$]	4820
Data, restraints, parameters	5292, 0, 408
Goodness-of-fit on F^2	1.045
Wavelength (Å)	0.71073
R, *R'* [$I > 2\sigma(I)$]*	0.0344, 0.0304
wR, *wR'* [$I > 2\sigma(I)$]*	0.0854, 0.0828
Maximum shift/esd	0.001
$\Delta\rho_{max, min}$ (e·Å^{-3})	0.800, −0.724

$w = 1/[\sigma^2(F_o^2) + (AP)^2 + BP]$, $P = (F_o^2 + 2F_c^2)/3$; R, $R' = \Sigma|F_o - F_c|/\Sigma|F_c|$, wR, $wR' = [\Sigma w(F_o^2 - F_c^2)^2/\Sigma w(F_o^2)^2]^{1/2}$ (ref. 9)

*3.2.3.5 Crystal structure of [Cu(**13a**)]·2H₂O*

On prolonged standing of the [Cu(**13**)] complex aqueous solutions on air the coordinated diphosphinate ligand was oxidised and the Cu^{II} complex of the appropriate diphosphonate crystallised out of the system. In this complex the copper central atom is surrounded by six donor atoms in a distorted octahedral coordination sphere with two oxygen atoms from the phosphonate groups being located in *cis*-positions (Fig.3.9). Distortion of the octahedron in the direction to one of the phosphonate moieties is relatively large. The axial Cu–O11 distance (2.716 Å) is approx. 0.7 Å longer than the equatorial Cu–O21 distance (1.981 Å), suggesting only a weak interaction between the N4-bound methylphosphonate group and the central Cu^{II} atom. The difference in strength of coordination binding of the respective phosphonate groups can also be seen in bond parameters of the phosphonate groups (cf. Table 3.8).

The Cu–N distances range from 2.051 to 2.207 Å (see Table 3.9). In the neutral complex the ligand is present in its double-deprotonated form, each of the methylphosphonate pendant arms bearing one negative charge. In the crystal lattice the molecules are interconnected by system of hydrogen bonds, either between two phosphonate groups from different ligand molecules or involving the solvate water molecules (Table 3.10).

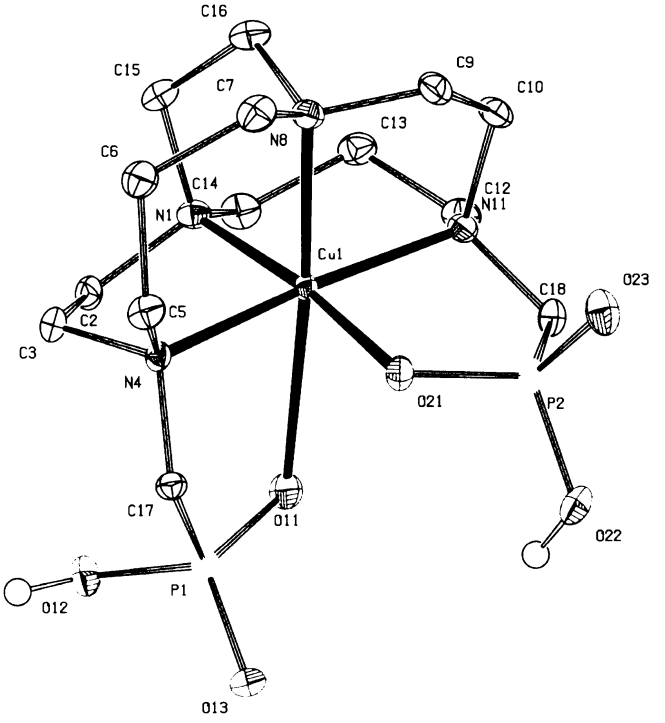

Fig.3.9 – The ORTEP view of complex [Cu(**13a**)] with 50 % thermal probability ellipsoids (carbon-bound hydrogen atoms and solvate molecules omitted for clarity)

The crystal, data collection and structure refinement details are given in Table 3.11.

*Table 3.8 – Structural parameters of the phosphonate moieties in the [Cu(**13a**)] complex (distances (Å) and angles (deg))*

P1–O11	1.5052(14)	P1–O12	1.5803(15)
P1–O13	1.5008(14)	O11–P1–O12	107.70(9)
O11–P1–O13	117.59(8)	O12–P1–O13	110.64(8)
P2–O21	1.5196(14)	P2–O22	1.5800(16)
P2–O23	1.4873(15)	O21–P2–O22	110.66(8)
O21–P2–O23	117.45(8)	O22–P2–O23	107.62(9)

Table 3.9 – Selected bond distances (Å) and angles (deg) in the [Cu(**13a**)] complex

Cu1–N1	2.0449(17)	Cu1–N4	2.0508(15)
Cu1–N8	2.2073(16)	Cu–N11	2.1041(16)
Cu1–O11	2.7160(15)	Cu1–O21	1.9808(14)
N1–Cu1–O21	173.30(6)	N4–Cu1–N11	176.02(7)
N8–Cu1–O11	173.84(6)	N1–Cu1–N4	85.55(6)
N1–Cu1–N8	86.07(7)	N1–Cu1–N11	97.71(7)
N1–Cu1–O11	87.81(6)	N4–Cu1–O11	79.93(5)
N4–Cu1–O21	88.43(6)	N4–Cu1–N8	98.84(6)
N8–Cu1–O21	86.07(7)	N8–Cu1–N11	83.69(6)
N11–Cu1–O11	97.87(5)	N11–Cu1–O21	88.19(6)
O11–Cu1–O22	88.26(5)		

Table 3.10 – Hydrogen bonds lengths (Å) in crystal structure of the [Cu(**13a**)]·5H_2O

O11#···H12O	1.757	O11#···O12	2.573
O1W···H22O	1.690	O1W···O22	2.600
O13@···H1W1	1.915	O13@···O1W	2.819
O13···H1W2	1.949	O13···O1W	2.762
O23···H2W1	1.986	O23···O2W	2.822
O23*···H2W2	2.222	O23*···O2W	2.927

x, –y+2, z+0.5; @ x, –y+2, z-0.5; * x, –y+1, z+0.5

Table 3.11 – X-ray crystal data collection and refinement details for complex [Cu(**13a**)]·2H_2O

	[Cu(**13a**)]·2H_2O
Empirical formula	$C_{14}H_{34}N_4O_8P_2Cu$
fw	511.93
Crystal shape	prism
Color	deep blue
Crystal system	monoclinic
Space group	*Cc* (No. 9)
a (Å)	15.0450(3)
b (Å)	14.8120(3)
c (Å)	9.1360(2)
α (deg)	90
β (deg)	100.3600(12)
γ (deg)	90
V (Å^3)	2002.73(7)
Z	4
ρ_{calc} (g·cm^{-3})	1.698
T (K)	293(2)
μ (mm^{-1})	1.302
F (000)	1076
θ range of data collection (deg)	1.95-27.49
Index ranges, *hkl*	−19 to 18, −19 to 19, −11 to 11
Reflections measured	4426
Reflections observed [$I > 2\sigma(I)$]	4368
Data, restraints, parameters	4426, 2, 287
Goodness-of-fit on F^2	1.086
Wavelength (Å)	0.71073
R, *R'* [$I > 2\sigma(I)$]^a	0.0213, 0.0209
wR, *wR'* [$I \geq 2\sigma(I)$]^a	0.0517, 0.0515
Maximum shift/esd	0.001
$\Delta\rho_{max,\ min}$ (e·Å^{-3})	0.279, −0.468

$w = 1/[\sigma^2(F_o^2) + (AP)^2 + BP]$, $P = (F_o^2 + 2F_c^2)/3$; R, $R' = \Sigma|F_o - F_c|/\Sigma|F_c|$, wR, $wR' = [\Sigma w(F_o^2 - F_c^2)^2/\Sigma w(F_o^2)^2]^{1/2}$ (ref. 9)

3.3 Experimental

3.3.1 General

The analytical grade chemicals were purchased from Lachema (Czech Republic), Fluka, Sigma-Aldrich or Merck and were used as received. All the reactions were carried out on air. Cyclam was prepared by slightly modified literature procedure,[11] using glyoxal hydrate trimer and Raney-Nickel. Cation exchange resin (Dowex 50, Fluka) and an anion exchange resin (Dowex 1, Fluka) were used for column chromatography.

Elemental analyses were conducted at the Institute of Macromolecular Chemistry of Academy of Sciences of the Czech Republic (Prague). Melting points were determined using a Kofler hot-stage apparatus (Boetius) and are uncorrected. NMR spectra were recorded on a Varian Unity Inova 400 spectrometer at 399.95 MHz for ^{1}H, 161.9 MHz for ^{31}P and 100.6 MHz for ^{13}C nuclei with internal references TMS for $CDCl_3$ solutions and *t*-BuOH for D_2O solutions, and external reference 85% H_3PO_4. The temperature (25 °C) was controlled by a VT-regulator, containing a thermocouple calibrated using MeOH and ethylene glycol according to a reported procedure. Multiplicity of the signals is indicated as follows: s – singlet, d – doublet, t – triplet, q – quintet, m – multiplet, b – broad. MS spectra were recorded on Bruker Esquire 3000 spectrometer equipped with electro-spray ion source and ion-trap detection in positive-ion mode.

3.3.1.1 Crystallography

The diffraction data were collected using a Nonius Kappa CCD diffractometer (Enraf-Nonius) at 293(2) and 150(2) K, respectively, using Mo-Kα radiation (λ = 0.71073 Å) and analysed using the HKL program package. The structures were solved using direct methods and refined by full-matrix least-squares techniques (SIR92 and SHELXL97). Scattering factors for neutral atoms were included in the SHELXL97 program. All non-hydrogen atoms were refined anisotropically. The hydrogen atoms were located in the electron density difference map; however they were fixed in theoretical or their original positions with thermal parameters U_{eq}(H) = 1.2 U_{eq}(C) or 1.3 U_{eq}(O,N), when the free refinement led to unreal bond lengths and/or extreme increase of number of refinement parameters.

3.3.2 Syntheses

*3.3.2.1 4,11-dibenzyl-1,4,8,11-tetraazabicyclo[6.6.2]hexadecane (**8a**)*

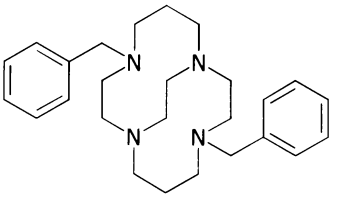

5 g (9 mmol) of perhydro-3a,8a-bis(phenylmethyl)-3a,5a,8a,10a-tetraaza-pyrenium dibromide monohydrate[5] was dissolved in 125 ml of EtOH/H_2O mixture (100 ml EtOH + 25 ml H_2O) at ambient temperature. To the stirred solution 2 g (53 mmol) of sodium borohydride ($NaBH_4$) were added and the mixture was stirred overnight at ambient temperature. The reaction was quenched by careful addition of 10% aq. HCl (30 ml) and the solvents were evaporated. The solids were dissolved in 50 ml of water and the pH of the solution adjusted to ~13 by addition of KOH. The product was extracted from this solution by benzene (3 x 40 ml), the organic phases were collected, dried over Na_2SO_4 and evaporated. Approx. 30 ml of acetone were added to the remaining colourless oil. The colourless crystals of the product precipitated out of the solution during 2 h. Directly from the preparation batch, the crystals for X-ray structure analysis were chosen. Yield 2.82 g (78 %).
ESI-MS: *m/z* [M+H^+] = 407; ^{1}H NMR ($CDCl_3$) δ (ppm): 1.32–1.43 (m, 2H, -CH_2-CH_2-CH_2-), 1.52–1.62 (m, 2H, -CH_2-CH_2-CH_2-), 2.28–2.52 (m, 12 H, incl. 2.46, d, 2H, N-CH_2-CH_2-N bridge), 2.85 (ddd, 2H), 3.18 and 3.78 (AB, 4H, -CH_2-Ph, *J* = 13.6 Hz), 3.96 (ddd, 2H), 7.19–7.36 (m, 10H).

*3.3.2.2 1,4,8,11-tetraazabicyclo[6.6.2]hexadecane (**8**)*

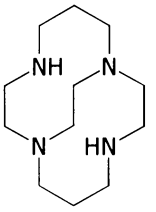

0.4 g of palladium on carbon (Pd/C, 10%, wet) were suspended in 60 ml of acetic acid and stirred under constant flow of hydrogen for 1 h. To the suspension of activated catalyst solution of 2 g of intermediate **8a** in 15 ml of acetic acid was added and the mixture was stirred for 24 h under constant hydrogen flow. The catalyst was then filtered off, washed by 10 ml of acetic acid and the filtrate was evaporated. The resulting slightly yellow oil was dissolved in 20 ml of distilled water and the pH of the solution adjusted to ~13

by KOH. The product was extracted by benzene (3 x 25 ml), the organic phases were collected, dried over Na_2SO_4 and evaporated to yield the amine in form of colourless oil (1 g, ~90%), which was used directly in the next reaction step.

*3.3.2.3 4-(4-nitrobenzyl)-1,4,8,11-tetraazabicyclo[6.6.2]hexadecane (**9**)*

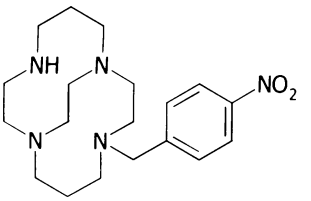

1 g of the amine **8** freshly prepared as described in 3.3.2.2 was dissolved in 80 ml of diethyl ether. 1 g of Na_2SO_4 was added to the solution and to this mixture the solution of 1.06 g (5 mmol) *p*-nitrobenzyl bromide in 80 ml of diethyl ether was added dropwise with stirring. Stirring of the heterogeneous mixture at ambient temperature was then continued for further 2 h. The bright yellow precipitate was then filtered off, washed by 20 ml of diethyl ether and air-dried. The yellow powder (containing the product and the drying agent) was extracted by 50 ml of chloroform and the yellow solution was evaporated under vacuum. The deep-yellow oil was dissolved in 15 ml of acetone and left for crystallisation in a fuming hood. The bright yellow crystals of the monohydrobromide formed after ~12 h were filtered off, washed with 5 ml acetone and dried under vacuum. Yield 1.9 g (87.6 %, based on **8a**). A single crystal selected from the preparative batch was used for the X-ray structure determination. MS-ESI *m/z* $[M+H^+]$ = 362; m.p. = 181–183 °C; ^{1}H NMR ($CDCl_3$) δ (ppm): 1.37–1.46 (m, 1H, -CH_2-C*H*-CH_2-), 1.63–1.85 (two overlapping m, 2H and 1H, -CH_2-C*H*$_2$-CH_2- and -CH_2-C*H*H-CH_2-), 2.37–2.45 (m, 3H), 2.52–2.94 (m, 14 H), 3.10 (ddd, 1H), 3.33 (bm, 1H), 3.35 (bm, 1H), 3.89 (AB, *J* = 14 Hz, 2H, -C*H*$_2$-Ar), 7.50–7.57 and 8.15–8.22 (AA'BB', 2H each, -*Ar*), 9.45 and 11.34 (N*H* and NH*H*$^+$); ^{13}C NMR ($CDCl_3$) δ (ppm): 21.35, 26.79, 44.49, 47.56, 49.97, 52.80, 52.83, 53.18, 53.33, 53.79, 55.52, 57.54, 58.80, 123.23, 130.93, 144.70, 147.05; Elem. anal. calcd. for $C_{19}H_{30}N_5O_2 \cdot HBr \cdot C_3H_6O$: C – 62.98 %, H – 8.89 %, N – 16.69 %; found: C – 63.05 %, H – 8.93 %, N – 16.47

*3.3.2.4 – 4,11-bis(4-nitrobenzyl)-1,4,8,11-tetraazabicyclo[6.6.2]hexadexane (**10**)*

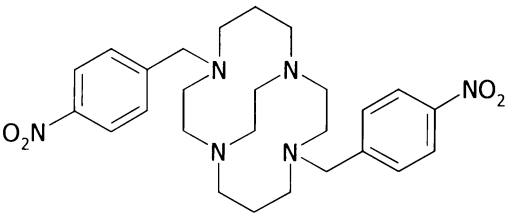

This compound could be isolated in minor amounts from the diethyl ether filtrate in the preparation 3.3.2.3 or was prepared as follows:

1 g of the amine **8** freshly prepared as described in 3.3.2.2 was dissolved in 25 ml of chloroform. To this solution 1 g of anhydrous Na_2CO_3 and solution of 2 g (9 mmol) of *p*-nitrobenzyl bromide in 15 ml of chloroform were added and the heterogenous mixture was stirred at ambient temperature for 2 h. The solids were filtered off and the solvent was evaporated under vacuum to yield 2.1 g of light yellow powder. This powder was recrystallised from acetone to yield light yellow crystals of the product (yield ~80 %, based on **8a**); m. p. = 229–230 °C (dec.); ESI-MS *m/z* [M+H$^+$] = 497; ^{1}H NMR ($CDCl_3$) δ (ppm): 1.35 (m, 2H, -CH_2-C*H*$_2$-CH2-), 1.49 (m, 2H,-CH_2-C*H*$_2$-CH_2-), 2.24–2.86 (m, 16 H), 3.06 (ddd, 2H), 3.26 and 3.76 (AB, 4H, -C*H*$_2$-Ar), 3.95 (ddd, 2H, *J* = 14.4 Hz), 7.42–7.46 and 8.08–8.12 (AA'BB', 4H each,-*Ar*); ^{13}C NMR ($CDCl_3$) δ (ppm): 28.05, 51.98, 54.28, 56.54, 57.46, 57.67, 59.64, 123.37, 129.42, 146.88, 148.90; elem. anal. calcd. for $C_{26}H_{36}N_6O_4 \cdot 2HBr$: C – 47.43 %, H – 5.82 %, N – 12.76 %; found: C – 47.68, H – 5.94, N – 12.43

*3.3.2.5 [11-(4-nitrobenzyl)-1,4,8,11-tetraazabicyclo[6.6.2]hexadec-4-yl]acetic acid ethyl ester (**11a**)*

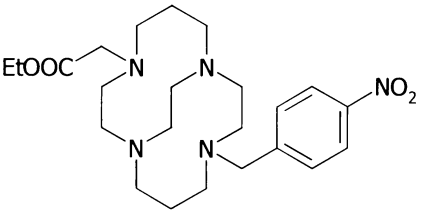

0.5 g (1 mmol) of **9**·HBr was dissolved in 30 ml of distilled water, the solution was made alkaline by addition of KOH and extracted with 3 x 10 ml of benzene. The organic fractions were collected, dried over Na_2SO_4 and evaporated under vacuum to yield an yellow oil of the free amine. This oil was dissolved in 25 ml of dry acetonitrile and to this solution 0.5 g of K_2CO_3 was added. To this mixture 0.4 g (2 mmol) of ethyl bromoacetate were added dropwise under stirring and the stirring was continued for next 24 h. The solvent was then removed under vacuum, the resulting oil dissolved in 30 ml of ice-cooled 0.5 M aq. NaOH and the product extracted with 3 x 20 ml of chloroform. The combined extracts were dried over Na_2SO_4 and evaporated under vacuum to yield 0.42 g (83 %) of light yellow powder; m. p. = 80–81 °C; ESI-MS *m/z* [M+H$^+$] = 448.6; ^{1}H NMR ($CDCl_3$) δ (ppm): 1.26 (t, 3H, *J* = 7.2 Hz, -CH_2-C*H*$_3$), 1.39 (m, 3H, -CH_2-C*H*$_2$-CH_2- and -CH_2-C*H*-CH_2-), 1.53 (m, 1H, -CH_2-C*H*H-CH_2-), 2.15–3.87 (set of overlapping multiplets, 24 H), 4.14 (q, 2H, *J* = 6.4 Hz, -C*H*$_2$-CH_3), 7.50 and 8.16 (AA'BB', 2H each, -*Ar*); ^{13}C NMR ($CDCl_3$) δ (ppm): 14.30, 27.43, 28.21, 51.15, 51.65, 52.79, 54.30, 54.65, 56.38, 56.54, 56.81, 57.22, 57.48, 59.17, 59.68, 60.09, 123.37, 129.36, 146.85, 149.13

*3.3.2.6 [11-(4-nitrobenzyl)-1,4,8,11-tetraazabicyclo[6.6.2]hexadec-4-yl]acetic acid (**11**)*

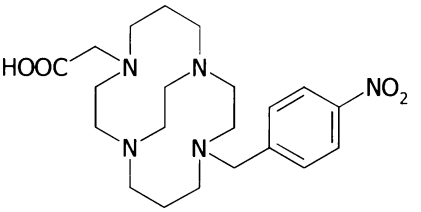

The ester **11a** was dissolved in 30 ml of 6 M aq. HCl and refluxed overnight. The solvent was removed under reduced pressure and the residue dissolved in 10 ml of 49 % aq. HBr. Hydrobromide of the product precipitated over several days on acetone vapour diffusion, the white powder was filtered off, washed with 10 ml of acetone and dried under vacuum. Yield 0.7 g (quant.). m. p. = 185–186 °C (dec.); ESI-MS *m/z* [M+H$^+$] = 420.5; ^{1}H NMR ($CDCl_3$) δ (ppm): 1.81 (m, 2H, -CH_2-C*H*$_2$-CH_2-), 2.43 and 2.56 (m, 1H, -CH_2-CH*H*-CH_2-), 2.66, (m, 1H), 2.82–4.06 (set of overlapping m, 21H), 4.81 and 5.03 (AB, *J* = 14 Hz, 2H, -CH_2-X), 7.84–7.87 and 8.32–8.35 (AA'BB', 2H each, -*Ar*); ^{13}C NMR ($CDCl_3$) δ (ppm): 16.93, 20.88, 46.49, 49.86, 50.43, 55.08, 55.57, 55.70, 55.73, 57.09, 59.26, 58.76, 59.26, 59.52, 125.11, 128.26, 135.00, 137.51, 150.41; Elem. anal. calcd. for $C_{21}H_{33}N_5O_4 \cdot 4HBr \cdot H_2O$: C – 33.14 %, H – 5.16 %, N – 9.20 %, found: C – 33.32 %, H – 5.25 %, N – 9.04 %

*3.3.2.7 [11-(4-nitrobenzyl)-1,4,8,11-tetraazabicyclo[6.6.2]hexadec-4-yl-methyl]phosphinic acid (**12**)*

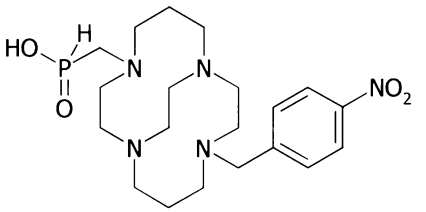

1 g (2 mmol) of compound **9**·HBr was dissolved in 30 ml of the ethanol/water mixture (1 : 1). To the solution several pellets of KOH were added, and the amine was extracted from this mixture by chloroform (3 x 10 ml). The combined extracts were dried with Na_2SO_4 and evaporated under vacuum. The resulting yellow oil was dissolved in 50 ml of 6 M aq. HCl and to this solution 1.5 g (20 mmol) of phosphinic acid and 0.2 g (4 mmol) of paraformaldehyde were added. The mixture was stirred at about 30 °C overnight. The solvents were removed under reduced pressure, the remaining oil dissolved in 10 ml of distilled water and chromatographed using cation-exchanging resin (Dowex 50, H^+-form) eluting the non-cationic impurities by distilled water and the product by 5 % aq. ammonia. The solvents from the collected fractions were removed under vacuum. The resulting oil was dissolved in 4 M ethanolic HBr and the product precipitated on slow addition of acetone. The hygroscopic off-white

product was filtered from the solution, washed with acetone and dried under vacuum. Yield 0.46 g (~30 %); ESI-MS *m/z* [M+H$^+$] = 440.6; ^{1}H NMR (D_2O) δ (ppm): 1.82 (m, 2H, -CH_2-C*H*$_2$-CH_2-), 2.32 (m, 2H, -CH_2-C*H*$_2$-CH_2-), 2.73–3.73 (set of overlapping m, 22H), 4.65 and 4.88 (AB, *J* = 13.6 Hz, -C*H*$_2$-Ar), 6.59 and 7.97 (d, $^1J_{P\text{-}H}$ = 552 Hz, 1H, P-*H*), 7.69–7.73 and 8.34–8.28 (AA'BB', 2H each, -*Ar*); ^{13}C NMR (D_2O) δ (ppm): 21.35, 21.67, 47.57, 50.04, 51.90, 51.96, 54.57, 55.18, 55.32, 55.44, 55.81, 57.69, 59.77, 60.20, 125.95, 135.15, 136.50, 150.40; ^{31}P NMR (D_2O) δ (ppm): 15.41 (d, $^1J_{P\text{-}H}$ = 552 Hz, *P*-H); Elem. anal. - due to extreme hygroscopicity of the product the analysis afforded unreproducible results

*3.3.2.8(11-hydroxyphosphinoylmethyl-1,4,8,11-tetraazabicyclo[6.6.2]hexadec -4-ylmethyl)phosphinic acid (**13**) and (1,4,8,11-tetrazabicyclo[6.6.2]hexadec-4-ylmethyl)phosphinic acid (**14**)*

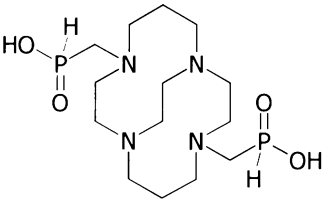

13

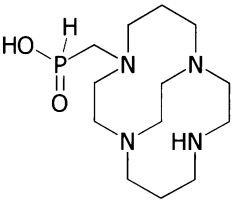

14

1 g of the oil of **8** freshly prepared as described in 3.3.2.2 was dissolved in 6 M aq HCl. To this solution 1.75 g (26.5 mmol) of phosphinic acid (H_3PO_2) and 265 mg (8.8 mmol) of paraformaldehyde were added and the mixture stirred at 30–40 °C for 24 h. The solvents were removed under vacuum (maximal bath temperature was set to 45 °C), the remaining oil was dissolved in 15 ml of distilled water and this solution chromatographed using cation-exchanging resin Dowex 50 in H$^+$-form. An excess of phosphinic acid (H_3PO_2) and other non-cationic byproducts were eluted by water, the product (together with monophosphinate derivative **14**) was eluted using 5 % aq. ammonia solution. The ammonia fractions were collected, evaporated under vacuum and re-chromatographed using anion-exchanging resin Dowex 1, eluting the monophosphinate **14** by water and the diphosphinate **13** by 10 % aq. acetic acid. The collected acidic fractions were concentrated under vacuum, the residual oil dissolved in 5 ml of ethanol and the product left for crystallisation on acetone vapour diffusion. Colourless crystals of the desired diphosphinic acid **13** were filtered, washed with ethanol and acetone and dried over P_4O_{10} in vacuum dessicator. Yield 0.34 g (16 % based on **8**); m.p. = 145–146 °C; ESI-MS *m/z* [M+H$^+$] = 383.0; ^{1}H NMR (D_2O) δ (ppm): 1.72 (m, 2H, -CH_2-C*H*$_2$-CH_2-), 2.32 (m, 2H, -CH_2-C*H*$_2$-CH_2-), 2.50 (m, 2H), 2.70 (m, 2H), 2.83 (m, 2H), 2.98–3.14 (set of m, 6H), 3.32–3.42 (m, 4H),3.62–3.82 (set of m, 8H), 6.53 and 7.90 (d, $^1J_{P\text{-}H}$ = 550 Hz, 1H, P-*H*); ^{13}C NMR (D_2O) δ (ppm): 21.55, 49.98, 53.00, 54.72, 55.56, 59.68, 60.59; ^{31}P NMR (D_2O) δ (ppm): 14.67 (d, $^1J_{P\text{-}H}$ = 550 Hz, *P*-H); Elem. anal. for $C_{14}H_{32}N_4O_2P_2 \cdot 5H_2O$ calcd.: C – 35.6 %, H – 8.9 %, N –

11.9 %, found: C – 35.4 %, H – 8.6 %, N – 11.6 %

The aqueous fraction from the second column chromatography was concentrated under reduced pressure. The remaining oil was dissolved in 5 ml of ethanol and the product precipitated by addition of about 30 ml of acetone. The white precipitate was filtered off, washed by acetone and dried under vacuum to yield ~ 50 mg of the monophosphinate derivative **14** as a white powder; ESI-MS *m/z* [M+H$^+$] = 304.9; ^{1}H NMR (D_2O) δ (ppm): 1.57–1.72 (m, 2H, -CH_2-C*H*$_2$-CH_2-), 1.90–2.04 (m, 2H, -CH_2-C*H*$_2$-CH_2-), 2.64 – 3.28 (set of overlapping m, 20H), 3.29–3.37 (m, 2H), 6.56 and 7.82 (d, $^1J_{P\text{-}H}$ = 504 Hz, P-*H*); ^{31}P NMR (D_2O) δ (ppm): 14.66 (d, $^1J_{P\text{-}H}$ = 504 Hz, *P*-H)

*3.3.2.9 Preparation of [Cu(**9**)Cl]Cl·2H$_2$O*

180 mg of **9** (obtained from the appropriate hydrobromide by chloroform extraction from aq. solution alkalised to pH~13 by KOH) was dissolved in 5 ml of methanol and to this mixture solution of 85 mg of $CuCl_2$·2H_2O in 5 ml of methanol was added. The deep blue solution was stirred at ambient temperature for 48 h and then refluxed for 3 h. The cooled solution was filtered and the filtrate placed into a desiccator filled by diethyl ether. Deep blued single crystals of the desired complex crystallised on overnight exposition of this solution to diethyl ether vapours.

*3.3.2.10 Preparation of [Cu(**13a**)]·2H$_2$O*

200 mg of diphosphinic acid **13** pentahydrate was dissolved in 5 ml of methanol and to this solution 72 mg of solid $CuCl_2$·2H_2O were added. The blue-green solution was refluxed for 5 h and the solvent evaporated under reduced pressure. The light-blue glassy residue was dissolved in 2 ml of distilled water and the solution was left for crystallisation. Repeated evaporation of water led to formation of light blue glassy solid unless the phosphinate moieties were oxidised by air to phosphonates (approx. 6 months). The single crystals of the product were isolated and used for X-ray structure determination.

3.4 Conclusions

Synthesis and characterisation of several 1,8-en-cyclam based ligands is reported. Synthesis of the symmetrically disubstituted derivative was achieved using procedures similar to those described in literature. The synthetic pathway leading to preparation of unsymmetrically substituted ligands is based on the low solubility of the mono-*p*-nitrobenzyl-substituted compound **9** hydrobromide in non-polar solvents, such as diethyl ether. This derivative was isolated in reasonable yields (~85–90 %), furnishing sufficient amounts of starting material for further derivatisation. The unsymmetrical precursors of bifunctional ligands were prepared in low to good yields using conventional reaction conditions.

Partial results of the compound **9** acid/base behaviour in aqueous media fulfil the expectations. Due to the potentiometric titration principal limits only two proton dissociation constants were observed, with the value of the last one close to 12. The ligating behaviour of this compound towards copper(II) exhibits a relatively sharp separation in the rate of the copper(II) incorporation depending on the pH value. While in the pH region above approximately 5 the complex seems to be formed after several hours at 50 °C, in the more acidic region (pH < 5) a complex formation was observed after several days of heating (80 °C) in a sealed ampoule.

Several attempts to prepare and isolate the copper(II) complexes of the unsymmetrical ligands bearing one acid pendant arm (**11** and **12**) failed. Although the formation of the complexes seems to proceed in the copper(II)/ligand solutions, only deeply coloured glassy solids were obtained on the crystallisation attempts involving various compensating anions, solvents and reaction conditions.

>-----<

References:

[1] T. J. Hubin, J. M. McCormick, S. R. Collinson, N. W. Alcock, D. H. Busch, *J. Chem. Soc., Chem. Commun.*, **1998**, 1657

[2] T. J. Hubin, J. M. McCormick, S. R. Collinson, N. W. Alcock, H. J. Clase, D. H. Busch, *Inorg. Chim. Acta*, **2003**, *346*, 76

[3] C. A. Boswell, X. Sun, W. Niu, G. R. Weisman, E. H. Wong, A. L. Rheingold, C. J. Anderson, *J. Med. Chem.*, **2004**, *47*, 1465

[4] X. Sun, M. Wuest, G. R. Weisman, E. H. Wong, D. P. Reed, C. A. Boswell, R. Motekaitis, A. E. Martell, M. J. Welch, C. J. Anderson, *J. Med. Chem.*, **2002**, *45*, 469

[5] E. H. Wong, G. R. Weisman, D. C. Hill, D. P. Reed, M. E. Rogers, J. S. Condon, M. A. Fagan, J. C. Calabrese, K.-Ch. Lam, I. A. Guzei, A. L. Rheingold, *J. Am. Chem. Soc.*, **2000**, *122*, 10561

[6] E. A. Lewis, R. W. Boyle, S. J. Archibald, *Chem. Commun.*, **2004**, 2212
[7] G. R. Weisman, E. H. Wong, D. C. Hill, M. E. Rogers, D. P. Reed, J. C. Calabrese, *J. Chem. Soc., Chem. Commun.*, **1996**, 947
[8] a) T. J. Hubin, N. E. Alcock, D. H. Busch, *Acta. Crystallogr., Sect. C: Cryst. Struct. Commun.*, **2000**, *56*, 37; b) T. J. Hubin, J. M. McCormick, S. R. Collinson, N. W. Alcock, H. J. Clase, D. H. Busch, *Inorg. Chim. Acta*, **2003**, *346*, 76
[9] G. M. Sheldrick, SHELXL97. *Program for Crystal Structure Refinement from Diffraction Data.* University of Göttingen, Göttingen, 1997
[10] A. Addison, T. N. Rao, J. Reedjik, J. van Rijn, G. C. Verschoor, *J. Chem. Soc., Dalton Trans.*, **1984**, 1349
[11] E. K. Barefield, F. Wagner, K. D. Hodges, *Inorg. Chem.*, **1976**, *15*, 1370; I. Meunier, A. K. Mishra, B. Hanquet, P. Cocolios, R. Guilard, *Can. J. Chem.*, **1995**, *73*, 685

>-----<

4. Conclusions

Two series of new bicyclic tetraazamacrocycles built up on skeletons of either 1,5,8,12-tetraazabicyclo[10.2.2]hexadecane (1,4-en-cyclam) **1** or 1,4,8,11-tetraazabicyclo[6.6.2]hexadecane (1,8-en-cyclam) **8** were prepared. The 1,4-en-cyclam-based unsymmetrical compounds bearing the *p*-nitrobenzyl moiety (precursor for a biomolecule-conjugation) were synthesised exploiting the low solubility of the intermediate quaternary derivative **2** in non-polar solvents. The ligands **3** and **6** exhibited the expected complexing ability towards copper(II) and zinc(II) although the complexation proceeded relatively slowly (at room temperature in order of hours). The metal complexes thus formed exhibited thermodynamic stability constants lower than those reported for similar monocyclic tetraazamacrocycles (cyclam, Me_4cyclam) probably due to inadvisability of the conformational change (chair or twisted-boat -> boat conformation of the piperazine subunit) connected to the metal ion encapsulation. On the other hand, when the stability of copper(II) complex of **3** is compared to stability constant reported for the bicyclic amine **1**, the trend in the values of these constants is the same for the couple ligand **1** – ligand **3** as for the couple cyclam – Me_4cyclam.

During the attempted synthesis of the monoacetate ligand **5a** an unusual reaction behaviour of **3** towards alkylation was observed. Reaction of the macrocyclic amine with alkyl bromoacetate agents lead (depending on the reaction solvent) to formation of either the quaternised monoacetate derivative **5** or quaternised diacetate derivative **4**. On the basis of molecular mechanics calculations, potentiometric titrations and multinuclear multidimensional NMR measurements (to establish the starting material **3** structure in solution) was this behaviour explained as a result of presence of a specific intramolecular hydrogen bond system forcing the first alkylation step on one of the piperazine ring nitrogen atoms (N1).

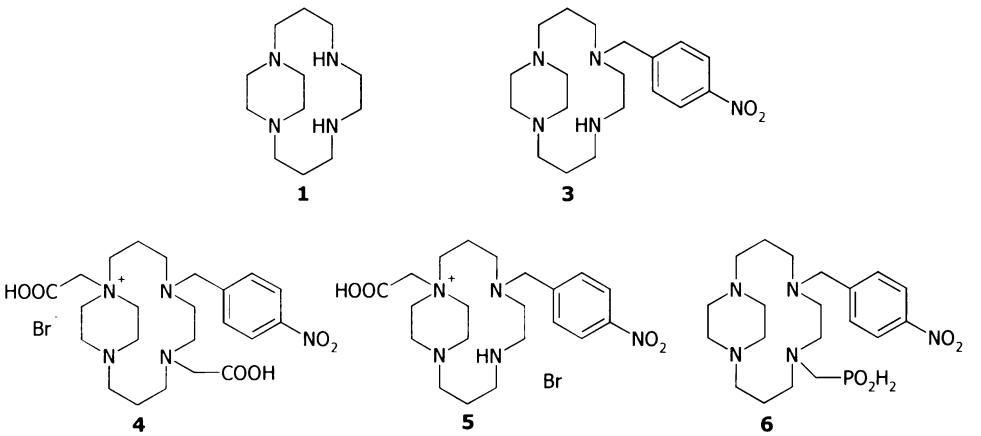

Fig. 5.1 – 1,4-en-cyclam and its derivatives mentioned in the text

The symmetrically substituted derivatives of 1,8-en-bridged cyclam were prepared either by use of common alkylating procedures (preparation of **10**) or by employing the Mannich-type reaction involving the phosphinic acid (H_3PO_2) as a substrate of this amino alkylation reaction (preparation of **13**) using the amine **8** as starting material.

The stepwise substitution on the 1,8-en-cyclam skeleton of **8** utilises the limited solubility of **9** hydrobromide in non-polar solvent (diethyl ether) which can be produced in excellent yield providing sufficient amounts of this starting material. Further substitution of **9** via alkylation using alkyl bromoacetate produces the appropriate acetate in form of its ester (**11a**) which is easily transformed to the acid (**11**). The Mannich-type reaction among **9**, phosphinic acid and paraformaldehyde produced the methylphosphinic derivative **12** in a low yield.

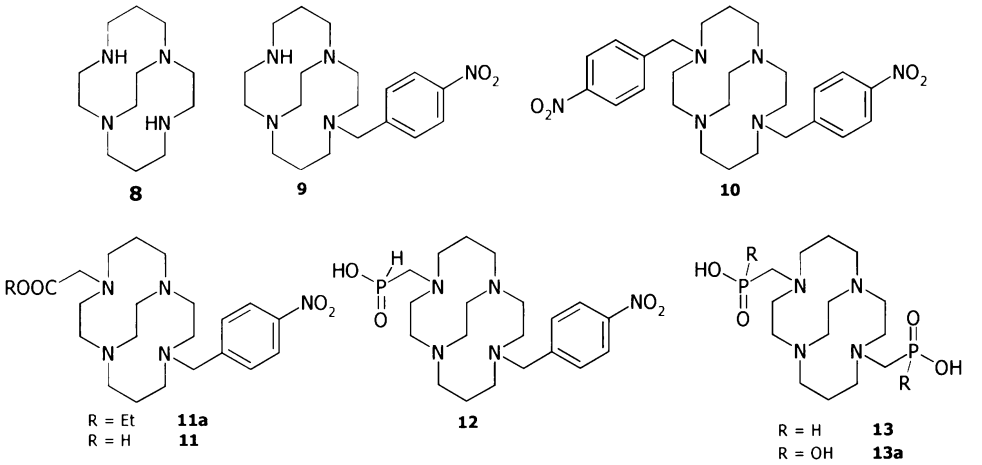

Fig. 5.2 – 1,8-en-cyclam and its derivatives mentioned in the text

All the prepared ligands can form coordination compounds with copper(II) but only few of them were isolated in the solid state, usually the complexes could be only isolated in form of intensively coloured glassy solids. The solid-state structures of copper(II) complexes with ligands **3**, **9** and **13a** have been determined using the single crystal X-ray structure determination method and the complexes exhibit the structural properties expected for this class of compounds.

Comparing the thermodynamic stability constants of copper(II) complexes of 1,4-en-cyclam-based ligands to the constants of similar complexes of 1,8-H_4te2p (Appendix I) results in a discovery that the new constrained macrocycles form copper(II) complexes with significantly lower thermodynamic stability constants than these cyclam-based ones. This observation can be explained involving energetics of the piperazine ring transformation during metal complex formation and the stabilisation effects of the methyl-phosphonate groups present in the H_4te2p ligand.

In addition, the kinetic inertness of Cu^{II} complexes with ligands **3** and **6** is not better than of the H_4te2p complex. The $[Cu(\mathbf{3})Br]^{2+}$ complex completely decomposed in acidic solution (1M $HClO_4$) during 24 hours at ambient temperature. Decomplexation of the ligand **6** from the appropriate Cu^{II} complex proceeded slower, after 10 d under the same conditions some complex (~20 %) was still present in the solution.

On the other hand, the 1,8-en-cyclam-based ligands represent a group of compounds with higher kinetic inertness expected. The ability and willingness of these ligands to form copper(II) complexes is probably strongly pH-dependent as no complex formation have been observed to pH ~5 at ambient temperature (the complex formation proceeds in a sealed ampoule at 80 °C in order of days) and a relatively good complexation proceeds at pH > 5 at slightly elevated temperature (50 °C, in order of hours) in the case of ligand **9**. A similar behaviour is supposed for ligands **11**, **12** and **13**.

All the presented results show that the ligands built either on the skeleton of 1,4-en-cyclam or 1,8-en cyclam are well suitable for copper(II) complexes formation. However, the ligands of the former groups, although they form copper(II) complexes very easily, seem not to be useful for the *in vivo* applications due to low stability of their copper(II) complexes. On the other hand, the ligands of the latter group form Cu^{II} complexes less readily and mostly under conditions not suitable for radioabelling of modified biomolecules but their kinetic inertness is supposed to be sufficient for the application into a living organism. For the purpose of the non-specific radiopharmaceuticals preparation is the 1,8-H_4te2p ligand of choice; for preparation of radiopharmaceuticals with more specific effect the bridged ligands could possibly represent a better alternative. Obviously, some more investigation, especially on copper(II) complexes formation / decomposition of the bridged macrocyclic ligands, is required to decide whether and with what limitations are the compounds of the invention useful for the radiomedicine.

Acknowledgements

To write down an objective acknowledgement seems to be the most difficult part of the thesis manuscript preparation...

First of all, the supervisors of this work should have been acknowledged – prof. Ivan Lukeš (our working group general supervisor) and doc. dr. Pet Hermann (directly supervising my work connected with elaboration of this thesis). Thanks for the introduction to the area of azamacrocycles and especially 'bridged' tetraazamacrocycles, which was necessary to my full re-orientation from the area of calix[4]arenes...

I also highly appreciate help of a number of my colleagues with some characterisations of the synthetic intermediates and products, namely assistance of Vojta Kubíček and Tomáš Vitha with the MS-spectra measurements and of Honza Kotek with solid state X-ray structures determinations. Also the virtually endless attempts to optimise the potentiometric titrations of Jana Havlíčková should have not been forgotten.

I'm obliged to point out the help of Honza Kotek with this manuscript final corrections – it is always difficult to find the appropriate mirror to selectively reflect one's thoughts; thanks a lot...

Non-replaceable part of the work was an open-minded atmosphere of the team I was participating in. Thanks to all the anonymous colleagues who formed it...

A scientist's life wouldn't be possible without a quiet place to live in and the loving family to live with. Many thanks belong to Linda for her love and patience and my children Anna, Viktorka and Tadeáš for their existence...

I also have to thank again to my parents, who, some years ago, didn't insist on me becoming a train dispatcher..

The research presented in this thesis was financially supported from the sources of the Grant Agency of the Czech Republic, Ministry of Education, Youth and Sport of the Czech Republic and the Charles University Grant Agency.